Original Article

MOLECULAR METABOLISM

Wntless regulates lipogenic gene expression in adipocytes and protects against diet-induced metabolic dysfunction

Devika P. Bagchi [1], Ziru Li [1], Callie A. Corsa [1], Julie Hardij [1], Hiroyuki Mori [1], Brian S. Learman [2], Kenneth T. Lewis [1], Rebecca L. Schill [1], Steven M. Romanelli [1], Ormond A. MacDougald [1,3,*]

ABSTRACT

Objective: Obesity is a key risk factor for many secondary chronic illnesses, including type 2 diabetes and cardiovascular disease. Canonical Wnt/β-catenin signaling is established as an important endogenous inhibitor of adipogenesis. This pathway is operative in mature adipocytes; however, its roles in this context remain unclear due to complexities of Wnt signaling and differences in experimental models. In this study, we used novel cultured cell and mouse models to investigate functional roles of Wnts secreted from adipocytes.

Methods: We generated adipocyte-specific Wntless (*Wls*) knockout mice and cultured cell models to investigate molecular and metabolic consequences of disrupting Wnt secretion from mature adipocytes. To characterize *Wls*-deficient cultured adipocytes, we evaluated the expression of Wnt target and lipogenic genes and the downstream functional effects on carbohydrate and lipid metabolism. We also investigated the impact of adipocyte-specific *Wls* deletion on adipose tissues and global glucose metabolism in mice fed normal chow or high-fat diets.

Results: Many aspects of the Wnt signaling apparatus are expressed and operative in mature adipocytes, including the Wnt chaperone Wntless. Deletion of Wntless in cultured adipocytes results in the inhibition of *de novo* lipogenesis and lipid monounsaturation, likely through repression of *Srebf1* (SREBP1c) and *Mlxipl* (ChREBP) and impaired cleavage of immature SREBP1c into its active form. Adipocyte-specific *Wls* knockout mice ($Wls^{-/-}$) have lipogenic gene expression in adipose tissues and isolated adipocytes similar to that of controls when fed a normal chow diet. However, closer investigation reveals that a subset of Wnts and downstream signaling targets are upregulated within stromal-vascular cells of $Wls^{-/-}$ mice, suggesting that adipose tissues defend loss of Wnt secretion from adipocytes. Interestingly, this compensation is lost with long-term high-fat diet challenges. Thus, after six months of a high-fat diet, $Wls^{-/-}$ mice are characterized by decreased adipocyte lipogenic gene expression, reduced visceral adiposity, and improved glucose homeostasis.

Conclusions: Taken together, these studies demonstrate that adipocyte-derived Wnts regulate *de novo* lipogenesis and lipid desaturation and coordinate the expression of lipogenic genes in adipose tissues. In addition, we report that Wnt signaling within adipose tissues is defended, such that a loss of Wnt secretion from adipocytes is sensed and compensated for by neighboring stromal-vascular cells. With chronic overnutrition, this compensatory mechanism is lost, revealing that $Wls^{-/-}$ mice are resistant to diet-induced obesity, adipocyte hypertrophy, and metabolic dysfunction.

Keywords Wntless; Wnt signaling; Adipose tissue; Lipogenesis; Adipocyte; Metabolism

1. INTRODUCTION

Wnts are members of an evolutionarily conserved family of secreted glycoproteins with established roles in cell proliferation and differentiation during tissue development [1,2]. When canonical Wnts bind to their membrane-spanning frizzled (Fzd) receptors and low-density lipoprotein receptor-related protein (LRP) co-receptors, they trigger an intracellular signaling cascade that stabilizes free cytosolic β-catenin, which then translocates to the nucleus and coactivates DNA-binding T cell factor/lymphoid enhancer-binding factor (TCF/LEF) proteins to

[1]Department of Molecular and Integrative Physiology, University of Michigan Medical School, Ann Arbor, MI, USA [2]Department of Microbiology and Immunology, University of Buffalo, Buffalo, NY, USA [3]Division of Metabolism, Endocrinology, and Diabetes, Department of Internal Medicine, University of Michigan Medical School, Ann Arbor, MI, USA

*Corresponding author. University of Michigan Medical School, Department of Molecular and Integrative Physiology, 1000 Wall Street, 6313 Brehm Tower, Ann Arbor, MI 48105, USA.

E-mails: dpbagchi@med.umich.edu (D.P. Bagchi), liziru@med.umich.edu (Z. Li), cscorsa@med.umich.edu (C.A. Corsa), julie.hardij@gmail.com (J. Hardij), morimori@med.umich.edu (H. Mori), bslearma@buffalo.edu (B.S. Learman), lewiskt@med.umich.edu (K.T. Lewis), rschill@med.umich.edu (R.L. Schill), smroma@med.umich.edu (S.M. Romanelli), macdouga@med.umich.edu (O.A. MacDougald).

Abbreviations: BAT, Brown adipose tissue; DNL, *de novo* lipogenesis; ER, Endoplasmic reticulum; eWAT, Epididymal white adipose tissue; HFD, High-fat diet; iWAT, Inguinal white adipose tissue; MSC, Mesenchymal stem cell; NCD, Normal chow diet; SVC, Stromal-vascular cells; SVF, Stromal-vascular fraction; TAG, Triacylglycerol; WAT, White adipose tissue; $Wls^{-/-}$, Adipocyte-specific Wntless knockout mice

Received February 12, 2020 • Revision received March 27, 2020 • Accepted April 2, 2020 • Available online 20 April 2020

https://doi.org/10.1016/j.molmet.2020.100992

mediate downstream gene transcription [1–3]. The endogenous Wnt pathway is a critical regulator of mesenchymal cell fat, inhibiting adipogenesis and promoting osteogenesis. [4–18].

Genetic studies in humans have also identified associations between Wnt pathway members and body fat distribution, obesity, and metabolic function. For example, genome-wide association studies across diverse human populations have found strong correlations between polymorphisms in the canonical Wnt transcriptional effector *TCF7L2* and susceptibility to type 2 diabetes [19–21]; indeed, *TCF7L2* is one of the strongest risk loci for development of type 2 diabetes. In addition, loss-of-function mutations in Wnt co-receptors *LRP5* and *LRP6* are associated with impaired glucose tolerance, osteoporosis, and cardiovascular disease [22,23], whereas gain-of-function *LRP5* mutations are associated with increased adiposity and altered fat distribution [24]. Common variants in Wnt signaling inhibitor *ZNRF3* and Wnt signaling activator *RSPO3* are associated with increased waist-to-hip ratio [25–27]. Further, gain-of-function mutations in *LGR4*, a protein that stabilizes Wnt receptors, are correlated with increased visceral adiposity [28]. Polymorphisms in the *SFRP5* locus have been associated with decreased adiposity in men [29], whereas missense variants in *WNT10B* and certain *WNT5B* single nucleotide polymorphisms are correlated with higher risk of obesity and type 2 diabetes, respectively [30,31]. Recently, variants in *CTNNB1* (β-catenin) have been linked to increased body mass index and risk of obesity [32]. Taken together, these studies provide strong genetic evidence for the influence of Wnt/β-catenin signaling on white adipose tissue (WAT) function, body composition, and metabolic health.

Although recent studies have demonstrated that Wnt signaling is active in mature adipocytes, its functional roles in this context remain unclear due to the complexity of the Wnt pathway and differences in experimental models, approaches, and results [13,14,32–34]. For example, stabilization of Wnt signaling through global deletion of secreted frizzled-related protein 5 (SFRP5), an adipocyte protein highly induced by obesity that binds to and sequesters Wnts, causes resistance to diet-induced obesity in mice [33]. Whereas total adipocyte numbers are unaffected, adipocytes in *Sfrp5* mutant mice have increased mitochondrial numbers and are smaller in size compared to control mice, resulting in reduced WAT and improved glucose tolerance. Adipocyte-specific deletion of β-catenin has also been reported to cause decreased subcutaneous WAT mass and improved glycemic control in diet-induced obese mice [32]. In contrast, adipocyte-specific deletion of the transcription factor *Tcf7l2* leads to adipocyte hypertrophy and impaired glucose homeostasis with diet-induced obesity [34]. These reports provide the first evidence that canonical Wnt signaling regulates ability of existing adipocytes to accommodate excess energy. Additional studies targeting the Wnt pathway in adipocytes are required to further understand how various components of this pathway differentially contribute to adipocyte metabolism.

Although it is clear that Wnt signaling is important within adipose tissues, one significant gap in our knowledge is the cellular source of physiologically relevant Wnts. To address this shortfall, we targeted Wntless (*Wls*), an evolutionarily conserved chaperone protein required for the transport of Wnts from the endoplasmic reticulum (ER) and Golgi apparatus to the cell membrane for secretion [35,36]. Wnt proteins are modified with palmitoleic acid (C16:1) at conserved serine residues, and the lipocalin-like structure of Wntless may facilitate binding to these hydrophobic modifications [37–41]. In fact, palmitoleoylation at Ser209 of Wnt3a mediates its physical binding to Wntless and subsequent release from the ER, and is thought to be required for Wnt activity [37,42,43]. Deletion of Wntless in vertebrate and invertebrate animal models results in phenotypes consistent with loss of Wnt function, suggesting that Wntless regulates signaling at the level of Wnt transport and secretion in signal-producing cells [36,44–50].

In this paper, we report that Wntless is expressed in mature adipocytes and that *Wls* deletion leads to reduced *de novo* lipogenesis (DNL) and lipid monounsaturation. Further, inhibition of a network of lipogenic genes is correlated with repression of *Srebf1* and *Mlxipl*, which encode SREBP1c and ChREBP, known transcriptional regulators of this gene set [51–53]. Of particular interest, in mice fed a normal chow diet (NCD), loss of adipocyte-specific Wnt secretion is defended by increased expression of Wnts in the surrounding stromal-vascular cells (SVC); however, this compensation is lost in mice fed a high-fat diet (HFD). Thus, $Wls^{-/-}$ mice challenged with long-term HFD demonstrate decreased adipocyte lipogenic gene expression, reduced size of epididymal adipocytes and WAT, and resistance to HFD-induced metabolic dysfunction. Studies from the cancer field have firmly established that inhibition of stearoyl CoA desaturase 1 (SCD1), which catalyzes the synthesis of palmitoleic acid, results in suppression of Wnt/β-catenin signaling [41,54–61]. Our studies reveal a reciprocal relationship in which Wnts are required for the expression of lipogenic genes and DNL, including the expression of SCD1 and formation of palmitoleic acid. Thus, these results highlight the novel and important roles of adipocyte-derived Wnts in critical mature adipocyte functions, including the accumulation of lipids in WAT with HFD.

2. MATERIALS AND METHODS

2.1. Animals

$Wls^{fl/fl}$ mice (#012888, Jackson Lab, Ellsworth, ME, USA), which harbor loxP sites flanking exon 1, were crossed with adiponectin (Adipoq)-Cre mice (#028020, Jackson Lab, Ellsworth, ME, USA) to generate $Wls^{fl/fl}$ or $Wls^{-/-}$ mice. The animals were housed in a 12 h light/12 h dark cycle with free access to water and food. For HFD studies, the mice were fed a rodent diet with 60 kcal% from fat (#12492, Research Diets, New Brunswick, NJ, USA). All of the animal studies were approved by and conducted in compliance with the policies of the University of Michigan Institutional Animal Care and Use Committee. The daily care of the mice was overseen by the Unit for Laboratory Animal Medicine at the University of Michigan.

2.2. Body composition

Fat, lean, and free fluid masses were estimated with a Bruker Minispec LF90II NMR (Bruker, Billerica, MA, USA) at the University of Michigan Mouse Metabolic Phenotyping Center.

2.3. Glucose and insulin tolerance tests

For glucose tolerance tests, mice were fasted for 16 h and then administered an intraperitoneal injection of glucose (1 mg/kg body weight). For insulin tolerance tests, mice were fasted for 6 h and then given an intraperitoneal injection of insulin (Eli Lilly, Indianapolis, IN, USA). Mice on NCD received 0.5 U insulin/kg body weight whereas mice on HFD were administered 1.0 U insulin/kg body weight. Blood was collected from the tail vein, and glucose concentrations were monitored 0, 15, 30, 60, and 120 min after intraperitoneal injection using a glucometer and Contour Next blood glucose strips (Bayer AG, Leverkusen, Germany).

2.4. Serum measurements

Blood was collected from the tail vein or by cardiac puncture at the time of harvest and allowed to coagulate on ice for 2 h. After centrifugation at 2,000 × *g* for 20 min at 4 °C, serum was transferred to a new tube and stored at −80 °C. ELISA was used to estimate the

concentrations of serum insulin (Crystal Chem USA, Elk Grove, IL, USA), adiponectin (R&D Systems Inc., Minneapolis, MN, USA), and leptin (PeproTech Inc., Rocky Hill, NJ, USA). Triacylglycerols (TAG) and total and free cholesterol were measured via colorimetric assays (Cayman Chemical, Ann Arbor, MI, USA, and Abcam, Cambridge, UK, respectively).

2.5. Adipocyte and stromal-vascular cell fractionation

Inguinal WAT (iWAT) and epididymal WAT (eWAT) were excised from the mice [62,63], minced with scissors, and digested for 1 h at 37 °C with shaking (600 rpm) in 2 mg/ml collagenase type I (Worthington Biochemical, Lakewood, NJ, USA) in Krebs-Ringer-HEPES (KRH; pH 7.4) buffer containing 3% fatty acid-free bovine serum albumin (BSA; Gold Biotechnology, St. Louis, MO, USA), 1 g/L glucose, and 500 nM adenosine. The resulting cell suspensions were filtered through 100 μm cell strainers and centrifuged at 100×*g* for 8 min to separate the stromal-vascular fraction (SVF) and buoyant adipocytes. The fractions were washed 2 times with KRH buffer containing 3% fatty acid-free BSA, 1 g/L glucose, and 500 nM adenosine. For immunoblot analyses, the fractions were subsequently washed 1 time with KRH buffer containing 0.5% fatty acid-free BSA, 1 g/L glucose, and 500 nM adenosine.

2.6. Histology

Soft tissues were harvested and fixed in 10% neutral buffered formalin overnight at 4 °C. Bones were fixed in 10% neutral buffered formalin for 24 h, rinsed with water, and decalcified in 14% EDTA (pH 7.4) for 14 days. Paraffin-embedded tissues were sectioned at 5 μm thickness and stained with hematoxylin and eosin (H&E) as previously described [64]. The stained sections were imaged using a Zeiss inverted microscope at 100× or 200× magnification.

2.7. Adipocyte histomorphometry

Adipocyte size and number were quantified from the WAT sections stained with hematoxylin and eosin. After digital processing, individual adipocyte cross-sectional areas were quantified using MetaMorph Microscopy Automation and Image Analysis Software 2.0 (Molecular Devices, Sunnyvale, CA, USA) as previously described [64]. To compare adipocyte sizes between genotypes, frequency distribution curves were generated with bin values as follows: bin range: 0 to 18,000 μm^2 and bin width: 500 μm^2. Non-linear curves were fit to the data to visualize frequency distribution patterns.

2.8. Cell culture

Primary mesenchymal stem cells (MSC) were isolated from the ears of wild-type C57BL/6J (Jackson Labs, Bar Harbor, ME, USA) or *Wls*$^{fl/fl}$ mice as previously described [33,65,66] and cultured at 5% CO_2. Subconfluent MSCs were maintained in DMEM:F12 medium (Thermo Fisher Scientific, Waltham, MA, USA) containing 10% fetal bovine serum (FBS; Sigma—Aldrich, St. Louis, MO, USA) and supplemented with 10 ng/ml recombinant basic fibroblast growth factor (PeproTech Inc., Rocky Hill, NJ, USA). At two days post—confluence, adipogenesis was induced with 0.5 mM methylisobutylxanthine, 1 μM dexamethasone, 5 μg/ml insulin, and 5 μM rosiglitazone in DMEM:F12 containing 10% FBS. From days 2—4 of differentiation, the cells were fed fresh DMEM:F12 medium containing 10% FBS, 5 μg/ml insulin, and 5 μM rosiglitazone. Thereafter, the cells were maintained in DMEM:F12 containing 10% FBS. Accumulation of neutral lipids in adipocytes was visualized with Oil Red-O staining [67]. Briefly, the cells were washed with phosphate-buffered saline (PBS), fixed in 0.5% glutaraldehyde in PBS for 5 min, incubated in Oil Red-O working solution for 10 min at room temperature with gentle agitation, and then washed 2 times with PBS. The total TAG accumulation was quantified by colorimetric assay (Cayman Chemical, Ann Arbor, MI, USA). Cells cultured for lipid composition analyses were differentiated from days 6—12 in DMEM:F12 containing 10% charcoal-stripped FBS (Sigma—Aldrich, St. Louis, MO, USA). Where indicated, confluent MSCs or day 12 adipocytes were treated with 20 ng/ml recombinant Wnt3a (R&D Systems Inc., Minneapolis, MN, USA) for 4 h prior to collection.

2.9. Genetic recombination in cultured cells

To induce gene deletion, *Wls*$^{fl/fl}$ adipocytes were treated with adenoviral GFP or adenoviral Cre recombinase (1×10^{10} viral particles/ml) in serum-free maintenance medium from days 4—6 of differentiation. Adenoviruses were obtained from the University of Michigan Vector Core. Genetic recombination was confirmed by PCR with a three-primer system. Primer sequences were as follows: P1, CTTCCCTGCTTCTTTAAGCGTC; P2, AGGCTTCGAACGTAACTGACC; P3, CTCAGAACTCCCTTCTTGAAGC; floxed band: 556 bp; and recombined band: 410 bp.

2.10. Cellular fraction for isolation of free cytosolic and membrane β-catenin

To evaluate the levels of free cytosolic β-catenin, confluent MSCs were treated for 4 h with 20 ng/ml recombinant Wnt3a (R&D Systems Inc., Minneapolis, MN, USA) and cellular fractionation was performed as previously described. Briefly, the cells were washed twice with cold PBS and homogenized using a BioVortexer mixer (Chemglass, Vineland, NJ, USA) in ice-cold buffer containing 10 mM Tris pH 7.4, 140 mM NaCl, 5 mM EDTA, 2 mM DTT, and 1:100 protease inhibitor cocktail (Sigma—Aldrich, St. Louis, MO, USA). The lysates were then centrifuged for 10 min at 500×*g* at 4 °C to remove cellular debris. The lysates were subsequently ultra-centrifuged at 100,000×*g* for 90 min at 4 °C to obtain the cytosolic (supernatant) and membrane (pellet) fractions. Protein concentrations of the cell fractions were measured by BCA protein assay (Thermo Fisher Scientific, Waltham, MA, USA) and β-catenin expression was measured by immunoblotting as described in Section 2.17 [6,68].

2.11. De novo lipogenesis (DNL) assay

Cultured adipocytes were incubated overnight in fresh serum-free DMEM:F12 medium prior to DNL evaluation. The cells were then incubated in fresh DMEM:F12 medium (containing 0.5 mM sodium pyruvate, 0.5 mM L-glutamine, and 2.5 mM glucose) supplemented with 1% fatty acid-free BSA containing 0.5 μCi [^{14}C]-acetate (PerkinElmer, Waltham, MA, USA) and 5 μM sodium acetate for 1, 2, 4, or 8 h at 37 °C. At the end of the indicated incubation times, adipocytes were harvested and lipids extracted for analyses by thin-layer chromatography and scintillation counting.

2.12. Insulin-stimulated glucose uptake

Cultured adipocytes were fasted for 6 h in Dulbecco's PBS (dPBS; without calcium, magnesium, phenol red; Thermo Fisher Scientific, Waltham, MA, USA) with 0.7% fatty acid-free BSA at 37 °C. Cells were washed once with dPBS. Adipocytes were then stimulated with 0, 2, 10, 20, or 100 nM insulin in dPBS containing 0.7% fatty acid-free BSA. After 30 min, 0.1 μCi/ml [^{14}C]-2-deoxy-glucose and 1 mM 2-deoxy-glucose was added per well and incubated for an additional 10 min. To measure background glucose uptake, 50 μM cytochalasin B (glucose transport inhibitor) was added to a subset of wells during the last 10 min of insulin stimulation. Glucose uptake was terminated with the addition of 2-deoxy-glucose to a final concentration of 20 mM. The

medium was aspirated and cells were washed twice with ice-cold PBS. Adipocytes were then lysed in 0.1% sodium dodecyl sulfate. Llysates were centrifuged for 10 min at 13,600 × *g*, and supernatants were transferred to new tubes. Radioactivity in the supernatant was measured using a scintillation counter, background glucose uptake was subtracted, and labeled glucose uptake was normalized to the protein concentration of lysed cells.

2.13. Lipid extraction for gas chromatography analyses

Cultured adipocytes were washed twice with PBS and then suspended in 500 μl of a 1:2.5 methanol/water mixture. The cell suspension was transferred to a borosilicate glass tube. Wells were rinsed with 500 μl of a 1:2.5 methanol/water mixture and the volume was transferred to the glass tube. Then 375 μl chloroform and 375 μl 0.9% NaCl were added to each tube, which were then vortexed vigorously and centrifuged at 2,500 rpm for 20 min at 4 °C. The lower organic chloroform layer containing total lipids was transferred to a new tube and stored at −20 °C until analysis.

2.14. Fatty acid composition by gas chromatography

Fatty acids within extracted lipids were derivatized into their methyl esters by trans-esterification with boron trifluoride-methanol as previously described [69]. The derivatized methyl esters were re-dissolved in a small volume of hexane and purified by thin-layer chromatography using n-hexane-diethyl ether-acetic acid (50:50:2, v/v/v) as the developing solvent. After development, plates were dried and sprayed with Premulin. Products were identified under ultraviolet light by comparing the retention flow of methyl heptadecanoate (C17:0) standard (retention flow, 0.67) applied side-by-side on the same plate. Methyl esters were extracted from thin-layer chromatography powder with diethyl ether, concentrated under nitrogen and re-dissolved in 100 μl hexane. Fatty acid compositions of the lipids were analyzed by gas chromatography (GC) as follows. Analysis of FAMEs was performed with 1 μl sample injection on an Agilent GC machine, model 6890N equipped with a flame ionization detector, an auto sampler, and ChemStation software for data analysis. An Agilent HP 88 with a 30 m GC column with a 0.25 mm inner diameter and 0.20 mm film thickness was used. Hydrogen was used as a carrier gas and nitrogen was used as a makeup gas. The analyses were conducted with a temperature programming of 125—220 °C. The fatty acid components within unknown samples were identified with respect to retention times of authentic standard methyl ester mixtures run side-by-side. Fatty acid components were quantified with respect to the known amount of internal standard added and the calibration ratio derived from each fatty acid of a standard methyl ester mixture and the methyl heptadecanoate internal standard. The coefficient of variation for GC analyses was within 2.3—3.7%.

2.15. Quantitative RT-PCR

Total RNA was purified from frozen tissue or cultured cells using RNA STAT-60 (Tel Test, Alvin, TX, USA) according to the manufacturer's instructions. One μg of total RNA was reverse-transcribed to cDNA using M-MLV Reverse Transcriptase (Invitrogen, Carlsbad, CA, USA). qRT-PCR was performed using a StepOnePlus System (Applied Biosystems, Foster City, CA, USA) with qPCRBIO Sygreen Mix (Innovative Solutions, Beverly Hills, MI, USA). Prior to use, all primers were validated with a cDNA titration curve and product specificity was confirmed by melting curve analyses and gel electrophoresis of the qPCR products. The expression of each gene was calculated using a cDNA titration curve within each plate and was then normalized to expression of peptidylprolyl isomerase A (PPIA) mRNA. The qPCR primer sequences are shown in Supplemental Table 1.

2.16. RNA sequencing (RNA-seq) analyses

Confluent MSCs or day 12 adipocytes were treated with 20 ng/ml recombinant Wnt3a (R&D Systems Inc., Minneapolis, MN, USA) or vehicle for 4 h prior to lysis and RNA isolation.

Total RNA was isolated and purified as described in Section 2.15. After DNase treatment, samples (n = 4 per condition) were submitted to the University of Michigan Advanced Genomics Core for quality control, library preparation, and sequencing on an Illumina Hi-Seq platform. Read files were downloaded and collated into a single .fastq file for each sample. The quality of the raw read data were assessed using FastQC (version v0.11.30) to identify data features that may indicate quality problems (low-quality scores, over-represented sequences, or inappropriate GC content). The Tuxedo Suite software package was used for alignment, differential expression analysis, and post-analysis diagnostics. Briefly, reads were aligned to the UCSC reference genome using TopHat (version 2.0.13) and Bowtie 2 (version 2.2.1). FastQC was used for a second round of quality control post-alignment to ensure that only high-quality data were input for expression quantitation and differential expression analyses. Differential expression analysis was conducted using two distinct methods: Cufflinks/CuffDiff and HTSeq/DESeq2 using UCSC build mm10 as the reference genome sequence. To generate lists of Wnt-related genes significantly regulated by adipogenesis or recombinant Wnt3a treatment, data were analyzed using GOrilla (Gene Ontology Enrichment Analysis and Visualization Tool) and the PANTHER Classification System. The Wnt Homepage (http://web.stanford.edu/group/nusselab/cgi-bin/wnt/) was also used to generate a list of established Wnt pathway genes. The complete RNAseq dataset was then mined to identify Wnt-related genes that are up- or down-regulated during adipogenesis or in response to Wnt3a.

2.17. Immunoblot analyses

Tissues were collected from mice and homogenized using a Bio-Vortexer mixer (Chemglass, Vineland, NJ, USA) in ice-cold lysis buffer (1% SDS, 12.7 mM EDTA, 60 mM Tris—HCl, and pH 6.8) containing 1:100 protease inhibitor cocktail (Sigma—Aldrich, St. Louis, MO, USA). Lysates were then centrifuged at 13,600 × *g* for 10 min at 4 °C. For WAT lysates, the top lipid layer was removed, and extracts were centrifuged again. Cultured cells were washed once with PBS and homogenized in lysis buffer containing 1:100 protease inhibitor cocktail. The lysates were then centrifuged at 13,600 × *g* for 10 min at 4 °C. The protein concentrations of cell or tissue lysates were measured byBCA protein assay (Thermo Fisher Scientific, Waltham, MA, USA). Lysates were diluted to equal protein concentrations in lysis buffer and Laemmli sample buffer, vortexed vigorously, and heated at 95 °C for 5 min. Cell or tissue extracts (20 μg) were separated by SDS-PAGE on 4—12% gradient polyacrylamide gels (Invitrogen, Carlsbad, CA, USA) and transferred to Immobilon PVDF membranes (Millipore, Billerica, MA, USA). Membranes were blocked in 5% non-fat dried milk in Tris-buffered saline with pH 7.4 containing 0.05% Tween-20 (TTBS) for 1 h at room temperature and then immunoblotted with the indicated primary antibodies (1:1000) in 5% BSA in TTBS overnight at 4 °C. Blots were probed with horseradish peroxidase-conjugated secondary antibodies (1:5000) diluted in 5% non-fat dried milk in TTBS for 1.5 h at room temperature and visualized with Clarity Western ECL Substrate (Bio-Rad, Hercules, CA, USA) or SuperSignal West Femto Maximum Sensitivity Substrate (Thermo Fisher Scientific, Waltham, MA, USA). A list of primary antibodies is shown in Supplemental Table 2.

2.18. Statistics

All data are presented as mean ± S.D. When comparing two groups, significance was determined using Student's two-tailed t-test. When comparing multiple experimental groups, an analysis of variance (ANOVA) was followed by post hoc analyses with Dunnett's or Sidak's test as appropriate. Differences were considered significant at $p < 0.05$ and are indicated with asterisks.

3. RESULTS

3.1. Wntless is expressed in mature adipocytes and upregulated by diet-induced obesity

Canonical Wnt signaling has previously been established as a significant endogenous regulator of adipogenesis [4]. Although recent studies have provided compelling evidence that this pathway also plays a role in the metabolism of adipocytes [32–34], particularly under obesogenic conditions, the contribution of adipocyte-derived Wnt proteins has not been directly studied in this context. To this end, we first evaluated whether Wntless, the chaperone protein required for secretion of Wnts, is expressed and regulated in cultured adipocytes and WAT. In cultured MSCs derived from wild-type C57BL/6J mice, the expression of *Wls* mRNA and protein was high in precursors, transiently repressed during differentiation, and elevated again in mature adipocytes (Figure 1A,B). As expected, mRNA and protein expression of the adipocyte marker *Adipoq* (adiponectin) increased during adipogenesis, whereas the expression of the preadipocyte marker *Dlk1* (Pref1) decreased (Figure 1A,B).

In addition to adipocytes, WAT contains myriad cell types, including preadipocytes, stromal cells, endothelial cells, and immune cells. These cells comprise the SVF of WAT and many have been shown to have active Wnt signaling in other contexts [5,6,70–72]. We measured *Wls* mRNA in fractionated eWAT and iWAT of C57BL/6J mice and found that it is expressed at higher levels in isolated adipocytes than in the SVF (Figure 1C). We then conducted immunoblot analyses on various mouse tissues and observed that Wntless is highly expressed in diverse adipose depots (Figure 1D) with relatively low abundance in the lungs and pancreas. Once we established that *Wls* is expressed in mouse adipose tissues, we explored whether its expression in WAT is regulated by nutritional or environmental challenges. We found that *Wls* gene expression in eWAT and iWAT is upregulated by diet-induced obesity (Figure 1E); notably, this increase in *Wls* expression occurrs specifically in the adipocyte fraction and not in the SVF of eWAT and iWAT (Supplemental Figure 1A). Further, *Wls* is specifically regulated by HFD feeding as its expression is not altered by acute fasting, fasting/refeeding, calorie restriction, or acute cold exposure (Supplemental Figure 1B). Wntless protein expression is also upregulated by diet-induced obesity in eWAT and iWAT (Figure 1F). We also queried the publicly available GTEx dataset to determine the distribution of *Wls* gene expression across male and female human tissues and found that *Wls* is expressed at higher levels in WAT depots when compared to liver or skeletal muscle (Supplemental Figure 1C). These data suggest that Wntless, which is expressed in adipocytes and induced by obesity, likely plays a metabolic role in these cells, particularly under obesogenic conditions.

3.2. Wnt/β-catenin signaling is operative in cultured adipocytes

Although previous studies have characterized in detail the mechanisms by which Wnt signaling represses adipogenesis of mesenchymal precursors and promotes alternative cell fates [4,5,15,17,18], the expression pattern and roles of Wnt-related proteins in mature adipocytes is less clear. RNA-seq analyses of cultured MSCs and differentiated adipocytes revealed that many Wnts are induced during adipogenesis, including *Wnt2b*, *Wnt4*, *Wnt5b*, *Wnt8b*, *Wnt9a*, and *Wnt9b* (Figure 1G). We also observed the induction of *Fzd4* and *Fzd9* receptors and constitutive expression of other pathway members, such as *Ctnnb1* (β-catenin), *Lrp5*, *Lrp6*, *Sfrp1*, *Dvl1, Dvl2*, *Dvl3, Wnt16*, *Wnt2*, and *Wnt7b* (Supplemental Figure 1D). Consistent with all major components of the signaling pathway being either induced or expressed constitutively, a number of downstream Wnt targets were elevated in mature adipocytes, including *Wisp1*, *Wisp2*, *Axin2*, *Tcf7l2*, and *Tcf7l1*, among others. Further, treatment of mature adipocytes with recombinant Wnt3a regulates many Wnt pathway genes involved in negative feedback, as well as many adipocyte genes (Figure 1H; data not shown). Taken together, these data indicate that the canonical Wnt signaling apparatus is operative in mature adipocytes.

3.3. Wntless deletion in cultured adipocytes inhibits DNL and lipid monounsaturation

To study the molecular functions of Wntless in adipocytes, we isolated and cultured MSCs from the $Wls^{fl/fl}$ mice. This model allowed us to conduct metabolic and mechanistic studies in cells derived directly from our mouse model. $Wls^{fl/fl}$ MSCs were differentiated into adipocytes using a standard adipogenic cocktail. At day four of differentiation, adipocytes were infected in serum-free medium with adenoviral GFP as a control or adenoviral Cre recombinase to induce *Wls* gene deletion. Adipocytes were allowed to recover following infection and analyzed at days 12 to 14 of differentiation (Figure 2A). Recombination of the floxed allele was confirmed by a 3-primer PCR system (Figure 2B). Both qPCR and immunoblot analyses of Cre-infected adipocytes showed efficient deletion of *Wls* at the mRNA (Figure 2C) and protein (Figure 2D) levels. Deletion of Wntless does not affect differentiation and lipid accumulation, as assessed by adiponectin protein expression (Figure 2D), phase-contrast microscopy and Oil Red-O staining (Figure 2E), and measurement of TAG (Figure 2F). To investigate whether Wnt signaling is altered by *Wls* deletion, we measured the expression of known targets and found that Wnt-induced genes, including *Axin2*, *Tcf7l2*, *Cmyc*, and *Ppard* are down-regulated, whereas Wnt-suppressed gene *Id2* is up-regulated in $Wls^{-/-}$ adipocytes (Figure 2G). The down-regulation of Wnt target genes in $Wls^{-/-}$ adipocytes is relatively mild, suggesting that other pathways contribute to basal expression of these genes.

Of note, *Ctnnb1* mRNA is not altered, which is consistent with its primary regulation through protein turnover [6,73]. Free cytosolic β-catenin, which is not bound to E-cadherins and comprises a very small and highly regulated proportion of total cellular β-catenin in preadipocytes, is the pool of β-catenin that mediates Wnt signaling [5,6,68,74]. Thus, we measured free cytosolic β-catenin as a surrogate for Wnt signaling downstream of adipocyte-derived Wnts. Compared to $Wls^{fl/fl}$ cells, we found that free cytosolic β-catenin is significantly lower (~33%) in $Wls^{-/-}$ MSCs at baseline (Figure 2H; quantified in Supplemental Figure 2A). Interestingly, free cytosolic β-catenin also appears to be lower in $Wls^{-/-}$ MSCs upon stimulation with Wnt3a, which may be secondary to desensitization of the Wnt signaling pathway in the absence of Wntless and secreted Wnts. In contrast, similar levels of membrane β-catenin are observed in control and $Wls^{-/-}$ MSCs (Figure 2H; quantified in Supplemental Figure 2A). These data suggest that Wnt signaling is active in mature adipocytes and impaired secretion of adipocyte-derived Wnts influences downstream signaling in an autocrine/paracrine manner.

Since Wntless functions to chaperone Wnt proteins from the ER and Golgi apparatus to the plasma membrane for secretion, we hypothesized that its deletion might influence the adipocyte proteome. We

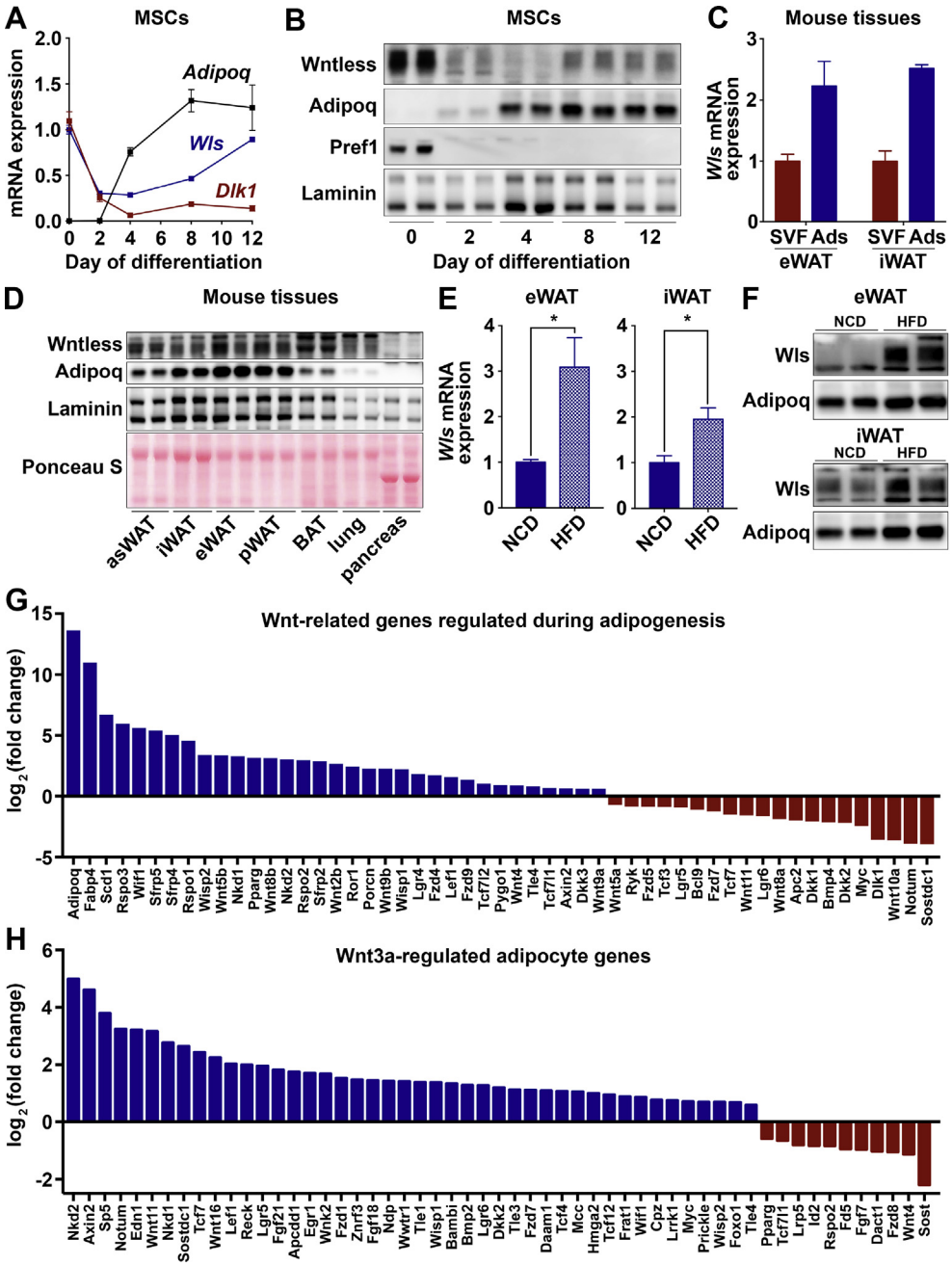

Figure 1: Canonical Wnt signaling is active in cultured adipocytes and Wntless is upregulated by diet-induced obesity. (**A**–**B**) MSCs isolated from C57BL/6J mice were cultured under standard conditions and induced to differentiate. Wntless gene (n = 6) and protein expression at indicated days of differentiation. (**C**) Wntless gene expression in the stromal-vascular (SVF) and adipocyte (Ads) fractions isolated from epididymal (eWAT) and inguinal (iWAT) white adipose tissues of C57BL/6J mice (males; n = 6). (**D**) Representative immunoblot of Wntless protein expression across C57BL/6J mouse tissues (asWAT, anterior subcutaneous WAT; pWAT, perirenal WAT; and BAT, brown adipose tissue); adiponectin, laminin, and Ponceau S were included as controls. (**E**–**F**) Regulation of Wntless gene and protein expression in eWAT and iWAT of 16-week-old wild-type mice fed a normal chow diet (NCD) or 8 weeks of high-fat diet (HFD) (males; n = 6). (**G**) Wnt-related genes found to be significantly up- or down-regulated by RNA-seq analyses of day 12 adipocytes vs day 0 cultured MSCs (n = 4). (**H**) Select Wnt-related genes found to be significantly up- or down-regulated by RNA-seq analyses of day 12 cultured adipocytes treated with recombinant Wnt3a (20 ng/ml) for 4 h (n = 4). RNA expression normalized to PPIA. Data are presented as mean ± S.D. * indicates significance at $p < 0.05$.

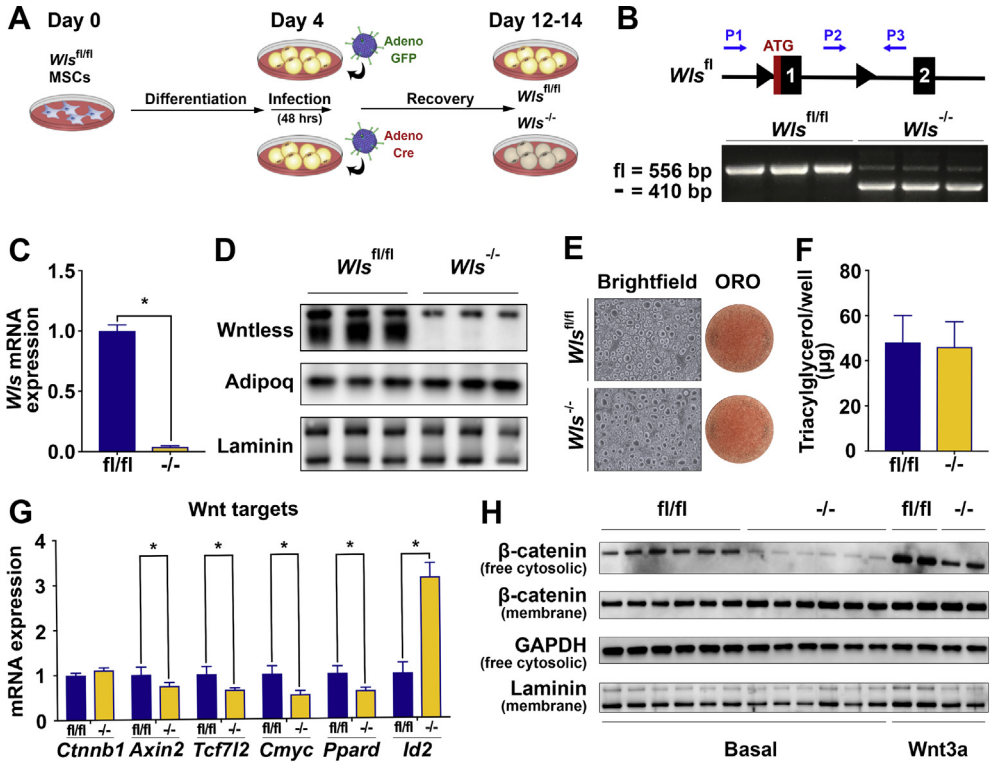

Figure 2: Wntless is required for canonical Wnt signaling in differentiated primary adipocytes. (**A**) Schematic model for deletion of Wntless in cultured adipocytes using adenoviral Cre recombinase. (**B**) Genetic recombination of Wntless in *Wls*$^{fl/fl}$ and *Wls*$^{-/-}$ adipocytes using a 3-primer PCR system (n = 3). (**C**–**D**) Wntless RNA and protein expression in adipocytes following adenoviral GFP or Cre infection (n = 3). (**E**) Representative brightfield and Oil Red-O images and (**F**) triacylglycerol accumulation in *Wls*$^{fl/fl}$ and *Wls*$^{-/-}$ adipocytes (n = 4). (**G**) Expression of known Wnt target genes in *Wls*$^{fl/fl}$ and *Wls*$^{-/-}$ adipocytes (n = 3). (**H**) Free cytosolic and membrane β-catenin protein expression in *Wls*$^{fl/fl}$ and *Wls*$^{-/-}$ confluent MSCs under basal conditions (n = 6) and after 20 ng/ml Wnt3a treatment for 4 h (n = 2); GAPDH and laminin shown as cytosolic and membrane loading controls, respectively. RNA expression normalized to PPIA. Data are presented as mean ± S.D. * indicates significance at $p < 0.05$.

therefore conducted untargeted proteomic analyses of *Wls*$^{fl/fl}$ and *Wls*$^{-/-}$ cultured adipocytes and observed substantial up- and down-regulation of adipocyte proteins (Supplemental Figure 2B). Of these potential Wnt targets, we focused our investigations on the down-regulation of SCD1, an important adipocyte enzyme in the ER that catalyzes the desaturation of palmitic (C16:0) and stearic (C18:0) acids into palmitoleic (C16:1, n-7) and oleic (C18:1, n-9) acids, respectively [75,76]. In addition to its role as the rate-limiting enzyme in fatty acid desaturation, SCD1 is also a key member of the DNL pathway (Figure 3A), which converts excess dietary carbohydrates and amino acids into fatty acids. A subset of these fatty acids are esterified to form TAG, which can later be hydrolyzed and fatty acids either secreted or metabolized by β-oxidation to provide energy for adipocytes and other cells in the body [77,78]. Consistent with proteomic data (Supplemental Figure 2B), we found that Wntless deficiency in adipocytes down-regulates the expression of *Scd1* mRNA (Figure 3A) and protein (Figure 3B). In addition, we also observed coordinate regulation of several enzymes involved in DNL and lipid metabolism (Figure 3A and B; quantified in Supplemental Figure 3A). Given the ~75% inhibition of SCD1 following *Wls* deletion, we hypothesized that *Wls*$^{-/-}$ adipocytes would have impaired fatty acid monounsaturation and therefore a larger proportion of saturated fatty acids. Thus, we next used GC to analyze the composition of esterified fatty acids in total lipids extracted from *Wls*$^{fl/fl}$ and *Wls*$^{-/-}$ adipocytes. Consistent with our hypothesis, we found that *Wls*$^{-/-}$ adipocytes contain a smaller proportion of monounsaturated fatty acids compared to *Wls*$^{fl/fl}$ adipocytes (Figure 3C). More specifically, compared to control adipocytes, differentiated *Wls*$^{-/-}$ cells contain higher levels of palmitic (C16:0) and stearic (C18:0) acids and lower amounts of myristoleic (C14:1, n-5), palmitoleic (C16:1, n-7), and vaccenic (C18:1, n-7) acids (Figure 3D–F). Of note, *Wls*$^{-/-}$ adipocytes contain mildly elevated levels of oleic acid (C18:1, n-9), consistent with previous reports of SCD1 inhibition in 3T3-L1 adipocytes [79].

In addition to SCD1, *Wls* deletion also regulates the expression of genes involved in lipid metabolism, including repression of ATP citrate lyase (*Acly*/ACLY), acetyl-CoA carboxylase (*Acaca*/ACC1), and fatty acid synthase (*Fasn*/FASN) (Figure 3A,B). We therefore conducted DNL assays using [^{14}C]-acetate to determine whether this pathway is less active in *Wls*$^{-/-}$ adipocytes. Cultured adipocytes were incubated in medium containing [^{14}C]-acetate for 1, 2, 4 or 8 h. Cells were then collected and lipids were extracted to measure radiolabel incorporation into TAG, diacylglycerol (DAG), and phospholipid (PL) fractions. Analyses of the conditioned media (Figure 3G) and whole cell lysates (Figure 3H) demonstrated that *Wls*$^{-/-}$ adipocytes take up less labeled acetate over time. Importantly, *Wls*$^{-/-}$ adipocytes incorporate significantly less radiolabel over time into the TAG fraction of cellular lipids (Figure 3I,J) but not the PL or DAG fractions (Figure 3I; quantified in Supplementary Figure 3B). Thus, downregulation of the DNL pathway secondary to Wntless deficiency is rate-limiting in adipocytes. Taken together, these data demonstrate that deletion of Wntless coordinately represses a network of lipogenic genes, thus altering the rate of lipogenesis and steady-state lipid composition in cultured adipocytes.

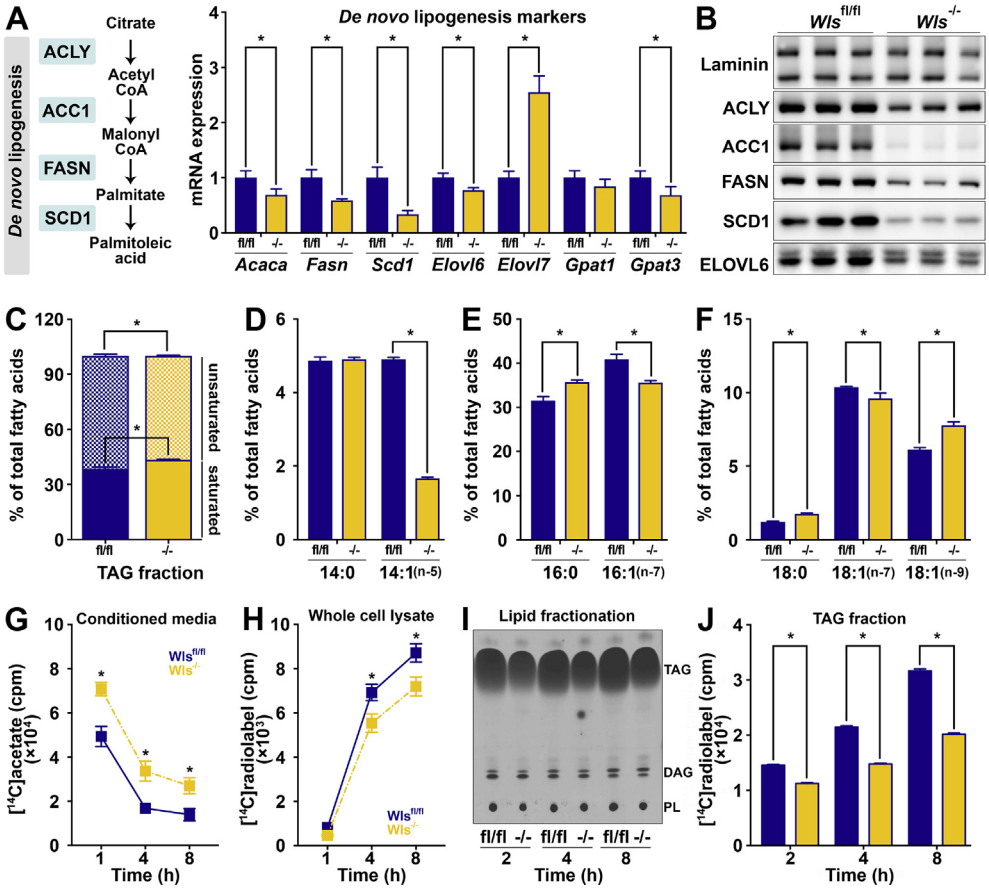

Figure 3: Adipocyte Wntless regulates the expression of a network of lipogenic genes and influences triacylglycerol fatty acid composition and *de novo* lipogenesis. (**A**–**B**) Lipogenic gene and protein expression in $Wls^{fl/fl}$ and $Wls^{-/-}$ adipocytes (n = 3). RNA expression normalized to PPIA. (**C**) Proportion of total saturated (solid) vs unsaturated fatty acids (hatched) in lipids extracted from $Wls^{fl/fl}$ and $Wls^{-/-}$ adipocytes (n = 6). Relative proportions of (**D**) myristatic (C14:0) vs myristoleic acid (C14:1), (**E**) palmitic (C16:0) vs palmitoleic acid (C16:1), and (**F**) stearic (C18:0) vs vaccenic (C18:1, n-7) or oleic acid (C18:1, n-9). *De novo* lipogenesis was evaluated in cultured $Wls^{fl/fl}$ and $Wls^{-/-}$ adipocytes using [^{14}C]-acetate for 1, 2, 4, and 8 h. [^{14}C]-radiolabel in (**G**) conditioned media vs (**H**) whole cell lysates after indicated incubation times was measured by scintillation counting (n = 3). (**I**) Representative thin-layer chromatography analysis of [^{14}C]-acetate incorporation into lipid species over indicated incubation times; TAG, triacylglycerol; DAG, diacylglycerol; and PL, phospholipid. (**J**) Radiolabel incorporation into TAG fractions extracted from $Wls^{fl/fl}$ and $Wls^{-/-}$ adipocytes was quantified by scintillation counting (n = 3). Data are presented as mean ± S.D. * indicates significance at $p < 0.05$.

3.4. Wntless regulation of lipogenic genes is likely mediated by SREBP1c and ChREBP and is independent of insulin responsivity

We next sought to understand the mechanism by which Wntless regulates the expression of *Scd1* and other lipogenic genes. In WAT and liver, sterol regulatory element-binding protein 1c (SREBP1c) and carbohydrate-responsive element-binding protein (ChREBP) are known key upstream transcriptional regulators of many genes involved in DNL, including *Acaca*, *Fasn*, and *Scd1* [51–53]. Thus, we explored whether these proteins are regulated in $Wls^{-/-}$ adipocytes. We found that expression of *Srebf1* and *Mlxipl*, which encode SREBP1c and ChREBP, respectively, are both down-regulated following the loss of Wntless, whereas other transcription factors involved in adipogenesis and adipocyte metabolism, including *Pparg*, *Lxra*, and *Lxrb*, are not influenced (Figure 4A). Although PPARγ protein was unchanged, *Cebpa* mRNA and protein were both slightly repressed in $Wls^{-/-}$ adipocytes, suggesting that this adipogenic transcription factor may also regulate lipogenic genes in mature adipocytes (Figure 4A, B). Importantly, immunoblot analyses revealed that SREBP1c and ChREBP proteins are both repressed in $Wls^{-/-}$ adipocytes (Figure 4B), which is of interest since the literature to date has not reported regulation by Wnt signaling of *Srebf1* or *Mlxipl* in mature adipocytes. In addition, SREBP1c is post-translationally cleaved at the ER and only mature, soluble SREBP1c translocates to the nucleus to mediate gene transcription. Of note, we observed that whereas the mature form of SREBP1c (~50 kDa relative mobility) is significantly decreased in the $Wls^{-/-}$ adipocytes, the larger immature form (~100 kDa) is reciprocally increased (Figure 4B,C). Taken together, these data suggest that Wntless regulates lipogenic gene expression through the expression of ChREBP, C/EBPα, and SREBP1c mRNA and proteins, with SREBP1c also potentially regulated at the post-translational level.

Previous studies have established insulin as an important regulator of *Srebf1* gene expression in the liver [80–83]. We therefore next investigated whether decreased responsivity to insulin mediates the effects of *Wls* deletion on SREBP1c and ChREBP in adipocytes. We first measured basal and insulin-stimulated glucose uptake and did not observe differences between $Wls^{fl/fl}$ and $Wls^{-/-}$ adipocytes (Figure 4D). We next assessed signaling downstream of insulin by immunoblot analyses and found that phosphorylation on specific serine or threonine amino acids in AKT was not impaired in $Wls^{-/-}$ adipocytes (Figure 4E). Although insulin has been shown to promote *Srebf1* mRNA expression in the liver, insulin treatment did not induce *Srebf1* or *Mlxipl* gene expression in either $Wls^{fl/fl}$ or $Wls^{-/-}$

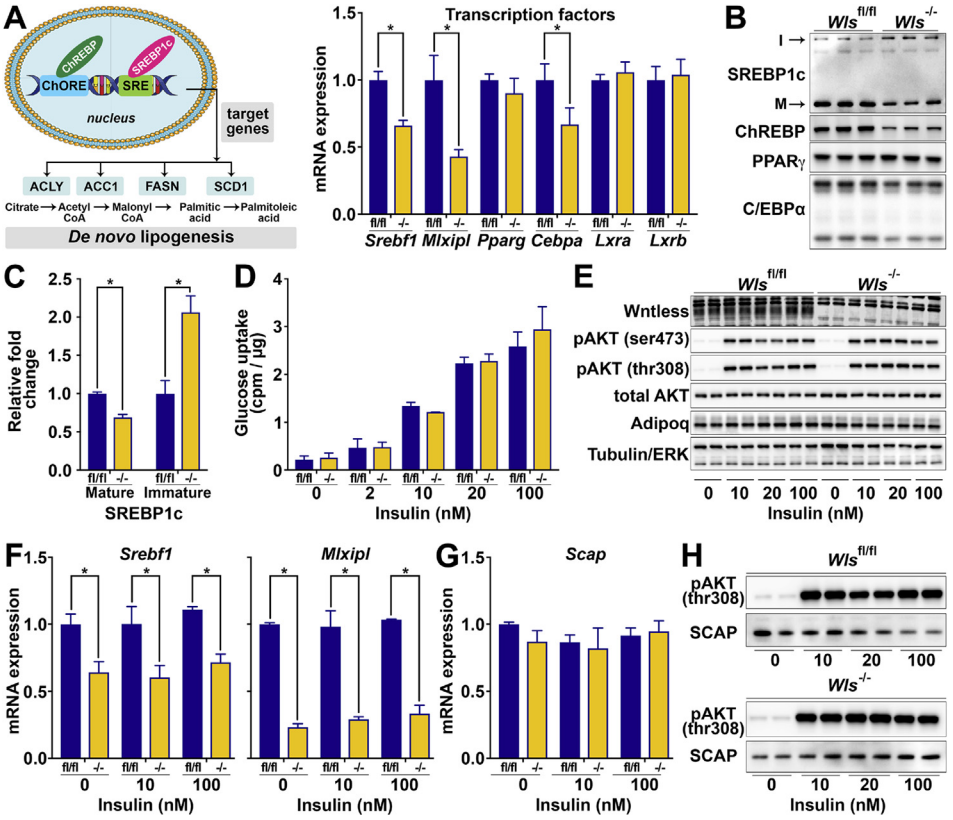

Figure 4: Wntless is required for the expression of *Srebf1* and *Mlxipl*, transcriptional regulators of lipogenesis. (**A**–**B**) Gene and protein expression of indicated transcription factors (n = 3); I: immature, insoluble form of SREBP1c at relative mobility of 100 kDa; and M: mature, soluble form of SREBP1c at 50 kDa. (**C**) Mature vs immature forms of SREBP1c quantified by densitometry. (**D**) Basal and insulin-stimulated glucose uptake into $Wls^{fl/fl}$ and $Wls^{-/-}$ adipocytes (n = 3). (**E**) Representative immunoblot of AKT phosphorylation in $Wls^{fl/fl}$ and $Wls^{-/-}$ adipocytes following treatment with indicated insulin concentrations for 10 min. (**F**) Expression of *Srebf1* and *Mlxipl* mRNAs in $Wls^{fl/fl}$ and $Wls^{-/-}$ adipocytes following treatment with indicated insulin concentrations for 24 h (n = 3). (**G**) Expression of *Scap* mRNA in $Wls^{fl/fl}$ and $Wls^{-/-}$ adipocytes following treatment with indicated insulin concentrations for 24 h (n = 3). (**H**) Representative immunoblot of SCAP protein expression in $Wls^{fl/fl}$ and $Wls^{-/-}$ adipocytes following treatment with indicated insulin concentrations for 10 min; pAKT(thr308) is shown as a control for insulin response. RNA expression normalized to PPIA. Data are presented as mean ± S.D. * indicates significance at $p < 0.05$.

adipocytes (Figure 4F). After translation, SREBP1 is anchored to the ER by a protein complex that includes SREBP cleavage-activating protein (SCAP) and insulin-induced genes 1 or 2 (Insig1 or Insig2) [51,80,84–86]. The Insigs function to prevent the maturation of SREBP1. In response to stimuli, including insulin, Insig activity is decreased and SCAP escorts SREBP1 from the ER to the Golgi apparatus, where it is cleaved into a soluble and transcriptionally active form [86,87]. We therefore explored whether SCAP mRNA or protein expression is altered by *Wls* deletion but found both to be unchanged in $Wls^{-/-}$ adipocytes (Figure 4G,H). Taken together, these data support the conclusion that in adipocytes, Wntless regulates SREBP1c and ChREBP through mechanisms independent of insulin responsivity.

3.5. Adipose-specific Wntless deletion does not influence body composition or whole-body metabolism in mice on NCD

Our studies have thus far demonstrated that Wntless expression is promoted by diet-induced obesity, and Wntless deficiency suppresses a network of lipogenic genes and DNL and reduces fatty acid monounsaturation of adipocyte lipids. Thus, we hypothesized that Wntless plays an important role *in vivo* in the appropriate storage of circulating nutrients, particularly under obesogenic conditions. To test this hypothesis, we generated adipose-specific *Wls* knockout mice by crossing $Wls^{fl/fl}$ mice with adiponectin-Cre mice. Adiponectin-Cre has been established as a model to delete floxed genes specifically and efficiently in adipocytes [88]. In our model, genetic recombination of *Wls* is only observed in adipose depots, and not in other tissues, such as the liver, pancreas, and muscle (Figure 5A). As expected, we found that Wntless mRNA (Figure 5B) and protein (Figure 5C) are decreased in iWAT and eWAT of $Wls^{-/-}$ mice on NCD. Analyses of mRNA from fractionated WAT demonstrated that *Wls* deletion occurs specifically in the adipocyte fraction and not in the SVF of iWAT and eWAT depots (Figure 5D). We then explored possible metabolic phenotypes in $Wls^{-/-}$ mice and did not detect differences in body composition (Figure 5E), growth over time (Figure 5F), glucose tolerance (Figure 5G), or insulin sensitivity (Figure 5H). Consistent with these data, $Wls^{-/-}$ mice did not exhibit altered fed or fasted concentrations of blood glucose (Figure 5I), serum insulin (Figure 5J), adiponectin (Figure 5K), or TAG (Figure 5L). Tissue weights such as iWAT, eWAT, brown adipose tissue (BAT), or liver were not different between $Wls^{fl/fl}$ and $Wls^{-/-}$ mice (Figure 5M). Similar results were observed in female mice fed NCD (Supplemental Fig. 4). Histological analyses of tissues did not yield substantial differences in adipocyte size or number within iWAT, eWAT, perirenal WAT, or BAT (Figure 6A; data not shown). In addition, liver morphology was unchanged (Figure 6A).

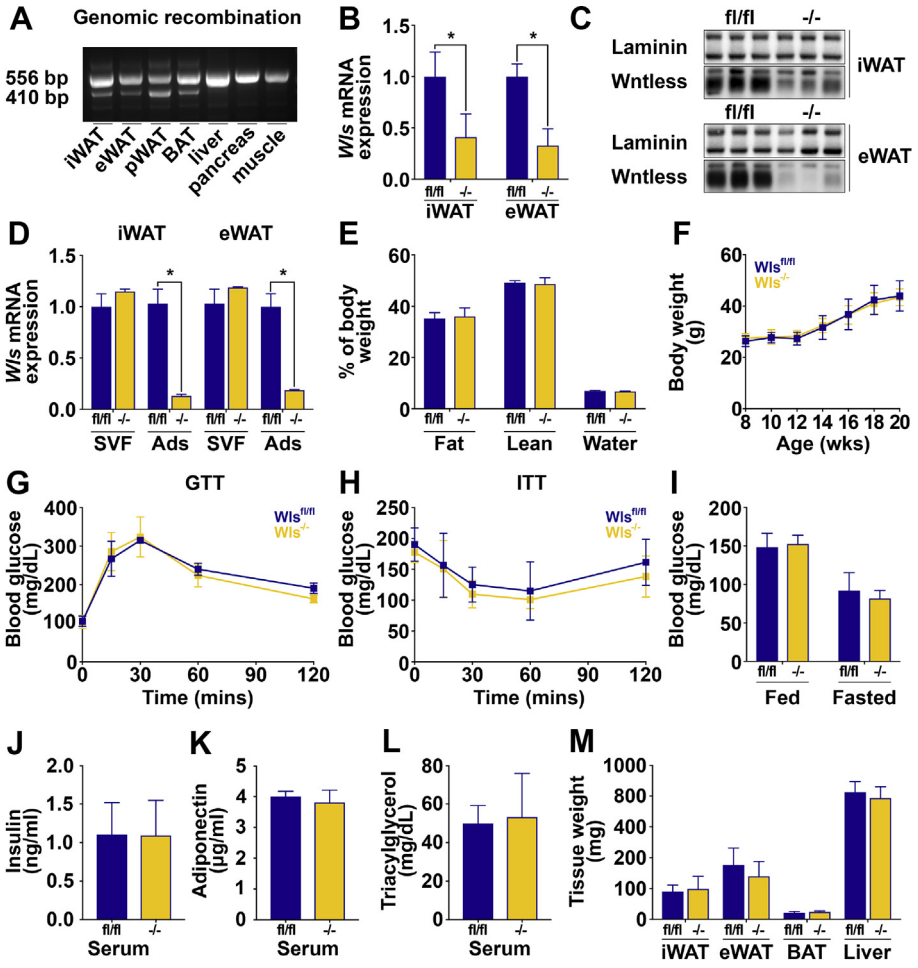

Figure 5: Adipose-specific Wntless deletion does not influence whole-body metabolism on a normal chow diet. (**A**) Genetic recombination of Wntless in tissues isolated from *Wls*$^{-/-}$ mice. (**B**—**C**) Wntless mRNA and protein expression in iWAT and eWAT of *Wls*$^{fl/fl}$ and *Wls*$^{-/-}$ mice. (**D**) Wntless mRNA expression in SVF and adipocytes isolated from iWAT and eWAT of *Wls*$^{fl/fl}$ and *Wls*$^{-/-}$ mice (n = 3). (**E**) Body composition of 16-week-old *Wls*$^{fl/fl}$ and *Wls*$^{-/-}$ mice on NCD. (**F**) Growth curve of 20-week-old *Wls*$^{fl/fl}$ and *Wls*$^{-/-}$ mice. (**G**) Glucose tolerance test in 16-week-old *Wls*$^{fl/fl}$ and *Wls*$^{-/-}$ mice. (**H**) Insulin tolerance test in 18-week-old mice. (**I**) Blood glucose concentrations in random-fed and 16 h fasted mice. Serum concentrations of (**J**) insulin, (**K**) adiponectin, and (**L**) triacylglycerols in 20-week-old mice. (**M**) Tissue weights at time of sacrifice. RNA expression normalized to PPIA. Data shown in E-M are from male mice, n = 5 per group. Data are presented as mean ± S.D. * indicates significance at $p < 0.05$.

Wnt signaling plays an important role in bone, where it increases bone mass and impairs marrow adiposity. For example, FABP4- or OCN-Wnt10b mice have extensive trabeculation throughout the entire endocortical compartment [15,16]. We therefore evaluated whether marrow cells traced by adiponectin-Cre are a critical source of Wnts in the bone marrow niche [89,90]. Histological analyses of tibias from both male and female cohorts suggest that Wntless deficiency does not influence the size or number of marrow adipocytes (Supplemental Figure 5A). In addition, micro-computed tomography (µCT) analyses indicate that cortical and trabecular bone mass variables are not influenced by *Wls* deletion (Supplemental Figure 5B—I).

Since Wntless was found to regulate lipogenic gene expression *in vitro*, we next measured the expression of a subset of key DNL genes in eWAT and iWAT of *Wls*$^{fl/fl}$ and *Wls*$^{-/-}$ mice. As expected, *Wls* gene expression is significantly decreased in both the eWAT and iWAT of *Wls*$^{-/-}$ mice (Figure 6B). Surprisingly, expression of most DNL pathway genes is not changed, with the exception of *Mlxipl* (Figure 6B). We also did not observe changes in DNL gene expression within the livers of *Wls*$^{-/-}$ mice (Supplemental Figure 6A). Analyses of isolated adipocytes from the *Wls*$^{-/-}$ mice showed that, despite efficient knockout of *Wls*, the expression of lipogenic genes is not altered (Figure 6C). This result was puzzling, so we next evaluated whether Wnt signaling is active within adipose tissues *in vivo*. To this end, we measured the expression of downstream Wnt target genes in isolated adipocytes and the SVF of *Wls*$^{-/-}$ mice and their *Wls*$^{fl/fl}$ counterparts, and found that expression of *Axin2* and *Id2* is dysregulated as expected in adipocytes with Wntless deficiency. Interestingly, for those adipocyte genes that are not suppressed as expected (*Cmyc*, *Tcf7l2*, and *Ppard*), compensatory Up-regulation is observed in the SVF (Figure 6D). Flow cytometric analyses of the SVF isolated from *Wls*$^{fl/fl}$ and *Wls*$^{-/-}$ mice did not reveal differences in subpopulation proportions (Supplemental Figure 6B and C); thus, we considered the possibility that SVCs of *Wls*$^{-/-}$ mice sense the adipocyte-specific loss of Wnt secretion and respond by increasing their own production to compensate for the deficiency. To this end, we measured the mRNA expression of many Wnts in the SVF isolated from *Wls*$^{fl/fl}$ or *Wls*$^{-/-}$ mice fed NCD and found significantly increased expression of several Wnts, including *Wnt6*, *Wnt9b*, *Wnt10a*, *Wnt10b*, and *Wnt16* (Figure 6E). We also observed decreased expression of *Wnt1*, *Wnt4*, and *Wnt8b*, whereas the expression of *Wnt2a*, *Wnt2b*, *Wnt3*, *Wnt5a*, *Wnt5b*, and *Wnt11* was unchanged. These data provide

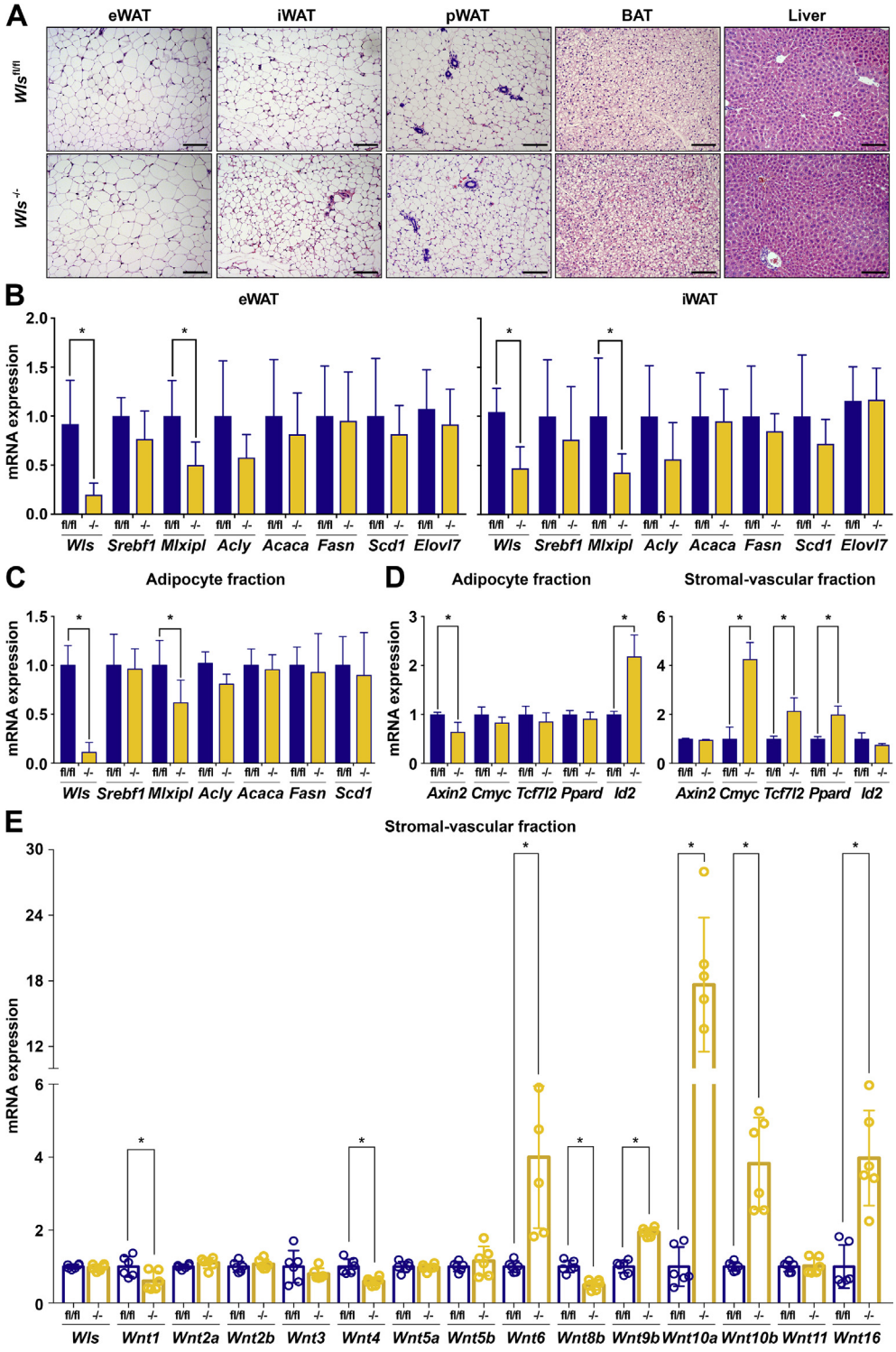

Figure 6: Adipose tissues compensate for adipocyte-specific Wntless deficiency by increasing Wnt signaling in stromal-vascular cells. (**A**) Representative histological images of H&E-stained tissues from *Wls*$^{fl/fl}$ and *Wls*$^{-/-}$ mice fed a normal chow diet for 20 weeks; 200× magnification; scale bar, 100 μm. (**B**) Lipogenic gene expression in eWAT and iWAT isolated from *Wls*$^{fl/fl}$ and *Wls*$^{-/-}$ mice. (**C**) Lipogenic gene expression in isolated eWAT adipocytes (n = 7). (**D**) Wnt target gene expression in isolated eWAT adipocytes and SVF of *Wls*$^{fl/fl}$ and *Wls*$^{-/-}$ mice (n = 5). (**E**) Expression of Wnt mRNAs in SVF isolated from eWAT of *Wls*$^{fl/fl}$ and *Wls*$^{-/-}$ mice (n = 6). Data shown are from male mice. RNA expression normalized to PPIA. Data are presented as mean ± S.D. * indicates significance at $p < 0.05$.

strong evidence for altered Wnt production by neighboring SVCs in response to impaired secretion from adipocytes. The dramatic induction of *Wnt6*, *Wnt9b*, *Wnt10a*, *Wnt10b*, and *Wnt16*, along with induction of Wnt target genes, suggests that WATs rigorously defend adipocyte-specific loss of Wnts by increasing signaling within SVCs.

3.6. *Wls*$^{-/-}$ mice on HFD have decreased adipocyte DNL gene expression, reduced size of epididymal adipocytes and WAT, and are protected from metabolic dysfunction

Previous studies have suggested that Wnt signaling plays an important role in the metabolism of adipocytes under conditions of nutrient excess [32–34]. We also found that the *Wls* expression is up-regulated within both subcutaneous and visceral WAT with diet-induced obesity (Figure 1E, F, and Supplemental Figure 1A). We therefore challenged *Wls*$^{fl/fl}$ and *Wls*$^{-/-}$ mice with 60% HFD for a minimum of 20 weeks and a striking metabolic phenotype emerged. Although HFD feeding did not cause a difference in body weight gain (Figure 7A), *Wls*$^{-/-}$ mice had decreased fat mass and increased lean mass (Figure 7B), which was not due to altered daily food intake (Supplemental Figure 7A). *Wls*$^{-/-}$ mice had significantly improved glucose tolerance (Figure 7C) and consistent with this, demonstrated higher random-fed (Figure 7D) and glucose-induced circulating insulin concentrations (Figure 7E) compared to the controls. Insulin sensitivity was not different (Figure 7F), nor were random-fed or fasting blood glucose concentrations (Figure 7G), serum leptin (Figure 7H), adiponectin (Figure 7I), TAG (Figure 7J), or free or total cholesterol (Figure 7K). Consistent with leaner body composition, eWAT weights of *Wls*$^{-/-}$ mice were decreased, whereas liver weights were increased (Figure 7L).

Histological analyses of *Wls*$^{-/-}$ tissues demonstrated significantly decreased eWAT adipocyte hypertrophy (Figure 8A,B) with a trend toward smaller cells observed in iWAT (Supplemental Figure 7B). The livers of *Wls*$^{-/-}$ mice showed improved hepatosteatosis (Figure 8A), likely contributing to the observed protection from glucose intolerance. Of note, we did not observe differences in histology of BAT or expression of UCP1 protein in *Wls*$^{-/-}$ mice (Supplemental Figure 7C), suggesting that the metabolic effects of Wntless deletion are not secondary to altered BAT thermogenesis. We next isolated the SVF and adipocytes from *Wls*$^{-/-}$ mice fed HFD and measured Wnt target

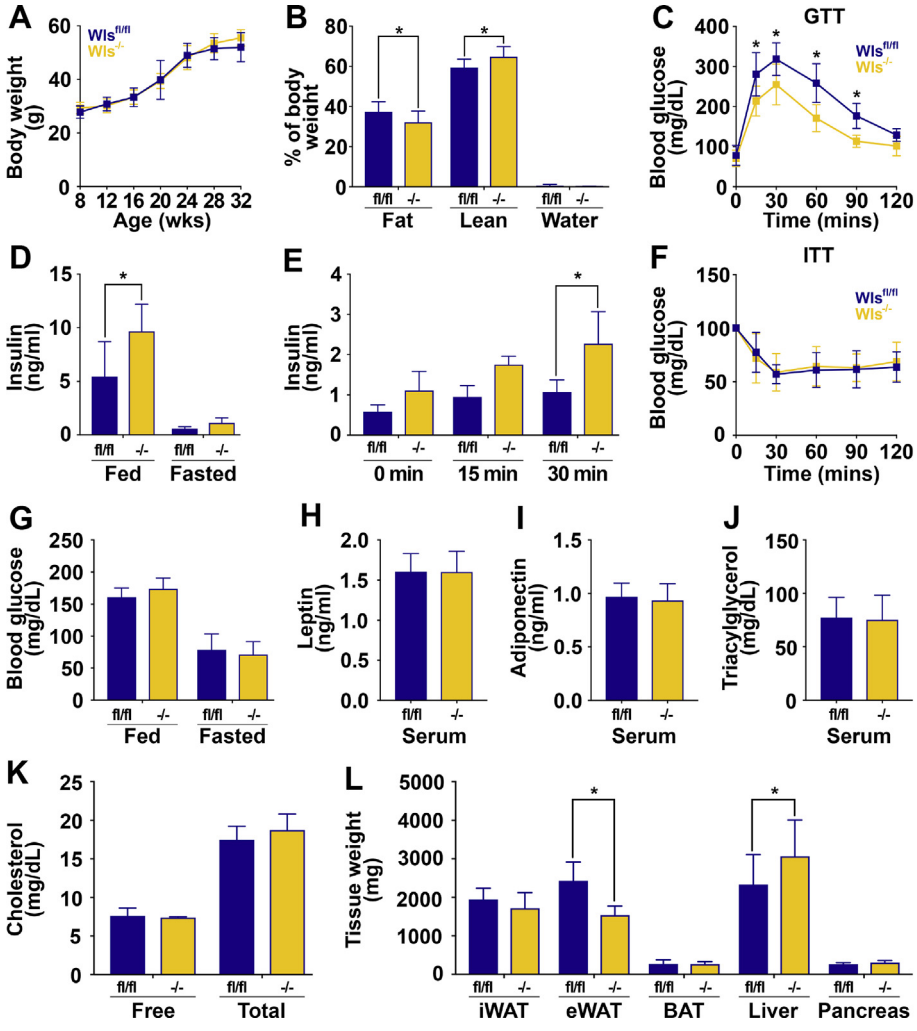

Figure 7: *Wls*$^{-/-}$ mice on HFD have decreased eWAT and improved glucose tolerance. (**A**) Growth curve over time of 32-week-old *Wls*$^{fl/fl}$ and *Wls*$^{-/-}$ mice fed 60% HFD for 24 weeks. (**B**) Body composition analysis of 28-week-old mice. (**C**) Glucose tolerance test in 28-week-old mice. (**D**) Serum insulin concentrations in fed and 16 h fasted mice. (**E**) Serum insulin concentrations in 16 h fasted mice at indicated times after intraperitoneal glucose injection (1 mg/kg body weight). (**F**) Insulin tolerance test in 30-week-old mice. (**G**) Blood glucose concentrations in random-fed and 16 h fasted mice. Circulating concentrations of (**H**) leptin, (**I**) adiponectin, (**J**) triacylglycerols, and (**K**) total and free cholesterol in 32-week-old mice. (**L**) Tissue weights of mice at time of sacrifice. Data shown are from male mice; *Wls*$^{fl/fl}$: n = 8; *Wls*$^{-/-}$: n = 7. Data are presented as mean ± S.D. * indicates significance at $p < 0.05$.

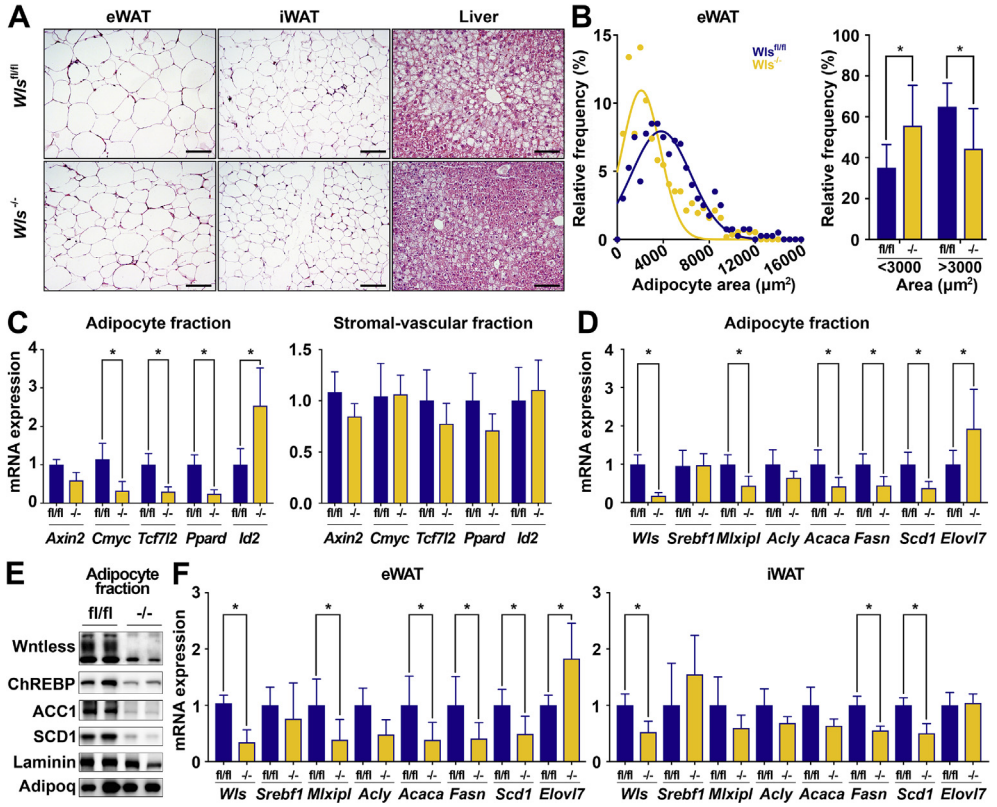

Figure 8: *Wls*$^{-/-}$ mice on HFD have reduced epididymal adipocyte size and decreased DNL gene expression. (**A**) Representative histological images of H&E-stained tissues from *Wls*$^{fl/fl}$ and *Wls*$^{-/-}$ mice f 60% HFD for 24 weeks; 200× magnification; scale bar, 100 μm. (**B**) Adipocyte size quantification of eWAT (400–500 adipocytes/mouse, n = 8 and 7). (**C**) Wnt target gene expression in adipocytes and SVF isolated from eWAT. (**D**–**E**) Lipogenic mRNA and protein expression in isolated eWAT adipocytes. (**F**) Lipogenic gene expression in eWAT and iWAT from *Wls*$^{fl/fl}$ and *Wls*$^{-/-}$ mice. Data shown are from male mice. RNA expression normalized to PPIA. Data are presented as mean ± S.D. * indicates significance at $p < 0.05$.

gene expression. We were intrigued to find that with HFD, the SVF of the *Wls*$^{-/-}$ mice no longer have elevated Wnt expression or downstream signaling (Figure 8C; Supplemental Figure 7D). Analyses of the adipocyte fraction showed that Wnt target gene expression is significantly decreased (Figure 8C), suggesting that HFD challenge diminishes the ability of WAT to maintain Wnt signaling homeostasis. Consistent with this result, the expression of several lipogenic genes, including *Mlxipl*, *Acaca*, *Fasn*, *Scd1*, and *Elovl7*, is coordinately regulated in isolated epididymal adipocytes (Figure 8D,E) and whole eWAT of *Wls*$^{-/-}$ mice (Figure 8F), in line with our studies in cultured adipocytes (Figures 3 and 4). A subset of these genes is also repressed in iWAT of *Wls*$^{-/-}$ mice (Figure 8F). To determine whether reduced WAT DNL is compensated for elsewhere, we isolated livers from the *Wls*$^{-/-}$ mice and found that they do not have altered DNL gene expression (Supplemental Figure 7E). In summary, our studies support the conclusion that with chronic overnutrition, adipose tissues of *Wls*$^{-/-}$ mice no longer defend Wnt signaling homeostasis, which leads to down-regulation of DNL enzyme expression, reduced adipocyte hypertrophy and adiposity, and overall improved metabolic health.

4. DISCUSSION

Extensive reports in the literature have characterized the mechanisms by which Wnt signaling in MSCs represses adipogenesis and promotes alternative cell fates, such as osteoblastogenesis [5,12,17,18,91]. The Wnts expressed in MSCs that function cell-autonomously include Wnt10b, Wnt10a, Wnt6, and other family members may conceivably participate as paracrine regulators [5,6,12]. The preponderance of evidence indicates that canonical Wnt/β-catenin signaling dominates control of MSC fate, with lesser contributions from the non-canonical pathway [5,91]. In this regard, the expression of β-catenin is suppressed during adipogenesis in both mouse and human models and its activity is further inhibited by induced expression of Wnt antagonist Chibby [92]. Much of the early data in this field focused on the inhibition of adipogenesis by Wnt signaling, and coordinate suppression of many genes involved in Wnt/β-catenin signaling during the early stages of differentiation. However, this study and other recently published reports demonstrate that repression of the canonical Wnt pathway during differentiation is transient, and that proteins including β-catenin, Wntless, and Tcf7l2, play important functional roles in mature adipocytes [32,34].

In this study, we report that essentially all aspects of the canonical Wnt signaling apparatus are expressed in mature adipocytes, including Wntless, Wnts, Fzd receptors, LRP co-receptors, Dishevelleds, β-catenin, TCF/LEFs, and modulatory proteins such as Axin2, SFRP4, and SFRP5. Indeed, Wnt signaling in cultured adipocytes is likely to have contributions from many Wnt proteins, including Wnt16, Wnt2, and Wnt7b, which are expressed at similar levels in MSCs and adipocytes, and Wnt2b, Wnt4, Wnt5b, Wnt8b, Wnt9a, and Wnt9b, which are induced during adipogenesis. These Wnts are proposed to act through LRP5 and LRP6 [9,10], in conjunction with Fzd4 and Fzd9, which also

increase during differentiation. We also observed induction of previously reported downstream Wnt targets WISP1 and WISP2, secreted adipokines that increase with obesity and are proposed to regulate whole-body insulin sensitivity [93,94]. In some cases, there may also be interspecies differences that will be important for our long-term understanding of these complex processes [95]. We showed that the core Wnt/β-catenin signaling molecules are expressed and operative within mature adipocytes, and expect that the unique combination of Wnts, receptors, and transcription factors provides distinct functional specificity; however, the cellular processes in adipocytes controlled by this pathway were previously poorly understood.

To evaluate the cell-autonomous functions of Wnt signaling in adipocytes, we blocked the secretion of adipocyte-derived Wnts through deletion of the Wnt chaperone protein, Wntless. As expected, Wntless deletion and presumed impairment of Wnt secretion from cultured adipocytes suppressed the accumulation of free cytosolic β-catenin and subsequent expression of several classic Wnt target genes, such as *Axin2*, *Tcf7l2*, and *Cmyc*, responses that have been observed in many other cell types. In the context of adipocytes, we observed that Wnt secretion is also required for coordinate expression of lipogenic genes, including *Acly*, *Acaca*, *Fasn*, and *Scd1*. Consistent with repression of these genes, *Wls*$^{-/-}$ adipocytes exhibit functional impairments in DNL and lipid monounsaturation. These effects on adipocyte metabolism are highly specific: Wntless deletion does not influence insulin-stimulated glucose uptake, adrenergic stimulation of lipolysis, or β-oxidation (Supplemental Figure 3C—E). These data are supported by Geoghegan *et al.*, who reported that *Tcf7l2* deletion in mesenchymal progenitors promotes adipogenesis and elevated expression of gene clusters involved in fatty acid and TAG metabolism [34], consistent with the repressive role of β-catenin and TCF/LEF signaling in this context [5]. Further, Tcf7l2 binding sites were reported within 1 kb of the transcriptional start site of most lipogenic genes, including *Acly*, *Fasn*, *and Scd1*, consistent with Wnt/β-catenin signaling directly coordinating adipocyte lipid metabolism [34].

A common feature of Wnt signaling in a wide range of cell types and animal models is inhibitory feedback, which provides an intricate restraint on Wnt-dependent gene activation [96,97]. Our lab previously observed Wnt1-induced feedback on members of the Wnt pathway in preadipocytes [98]; in this study, we uncovered a similar response to recombinant Wnt3a treatment of fully differentiated adipocytes. Thus, exogenous Wnt3a stimulates many of the classic inhibitory responses to limit the effects of Wnt signaling. These include induction of known feedback genes, such as *Nkd1*, *Nkd2*, *Axin2*, *Notum*, *Lgr5*, and *Tcf7*, coincident with repression of *Tcf7l2*, *Fzd8*, and *Lrp5*. Because Wnt secretion and functionality is largely dependent on lipid modification by SCD1-derived palmitoleic acid [41], inhibition of SCD1 results in reduced Wnt/β-catenin signaling, an observation extensively investigated in the cancer field [54—61]. In this study, we determined that the reciprocal relationship also holds true: endogenous Wnt signaling in adipocytes is required for lipogenesis and monounsaturation of lipids, including the formation of palmitoleic acid. Although signaling downstream of adipocyte Wnts is necessary for the maintenance of lipogenic genes and production of palmitoleic acid, stimulation of adipocytes with exogenous Wnt3a does not further promote the expression of these genes. These results may indicate that endogenous Wnt signaling plays a permissive role in the expression of lipogenic genes or perhaps that stimulation with a Wnt ligand other than Wnt3a may be necessary to observe dynamic regulation of this gene network.

In mice maintained on NCD, adipocyte-specific *Wls* deletion does not overtly influence body composition or whole-body metabolism. Consistent with our results, recent investigations into the role of Wnt signaling in mature adipocytes, including global deletion of *Sfrp5* or adipocyte-specific deletion of *Ctnnb1* or *Tcf7l2*, also did not yield metabolic phenotypes on a chow diet [32—34]. Although these previous studies did not further probe into a lack of detectable phenotypes, our experiments uncovered a novel compensatory mechanism by which adipose tissues defend the loss of adipocyte-derived Wnt signaling in mice fed NCD. We found that despite efficient Wntless ablation at the DNA, RNA, and protein levels, adipocytes isolated from *Wls*$^{-/-}$ mice do not have altered Wnt target or DNL gene expression. However, upon further investigation, we observed that SVF cells isolated from *Wls*$^{-/-}$ mice upregulate Wnt mRNAs, including *Wnt6*, *Wnt9b*, *Wnt10a*, *Wnt10b*, and *Wnt16*. Consistent with these data, we also found elevated Wnt target gene expression in *Wls*$^{-/-}$ SVCs, as evidenced by increased expression of *Cmyc*, *Tcf7l2*, and *Ppard*. These data suggest the intriguing possibility that under standard nutritional conditions, SVF cell populations sense the loss of adipocyte-derived Wnts and respond by up-regulating their own Wnt production and signaling to maintain downstream target gene expression within adipocytes.

Although mechanisms by which SVCs compensate for the loss of adipocyte Wnts is not yet clear, a number of possibilities exist. Wntless deficiency may alter the SVF cellular composition, enriching for subpopulations that have highly active Wnt signaling. However, flow cytometry analyses of immune, endothelial, and stromal cell proportions in the SVF did not yield observable differences between *Wls*$^{fl/fl}$ and *Wls*$^{-/-}$ mice, making this possibility less likely. Alternatively, a particular cell type in the SVF may detect the loss of Wnt signaling from adipocytes and compensate by increasing its own Wnt production and secretion. It is also possible that the intricate intracellular feedback mechanisms previously described may involve other families of secreted signaling molecules, including BMPs and FGFs, both of which are regulated in adipocytes by Wnt3a and have been shown in other contexts to interact with Wnt/β-catenin signaling [99—102]. Wnts are low-abundance, lipid-modified proteins that act locally in an autocrine/paracrine manner; these characteristics create major technical challenges for isolating and quantifying Wnts from the tissue or serum of *Wls*$^{fl/fl}$ and *Wls*$^{-/-}$ mice. Nevertheless, further studies will be necessary to fully elucidate the compensatory mechanisms by which specific SVF cells sense and respond to the loss of adipocyte-derived Wnt secretion.

Adipose tissues are critical for the maintenance of insulin sensitivity and glucose homeostasis through storage of excess energy and secretion of adipokines [63,103—106]. To date, the inhibition of adipose-specific Wnt signaling has been shown to influence whole-body glucose homeostasis under obesogenic conditions; however, discordant results have been reported between animal models that should, ostensibly, all be loss-of-function for Wnt signaling. For example, our work with *Wls*$^{-/-}$ mice found that more than 20 weeks of HFD overrides the compensatory Wnt signaling in adipose SVCs, revealing a striking phenotype. *Wls*$^{-/-}$ mice fed HFD are characterized by decreased fat and increased lean mass, improved glucose homeostasis, increased circulating insulin, and decreased lipogenic gene expression within WAT depots. Interestingly, these mice exhibit increased liver weight but improved hepatosteatosis by histological analysis. Although highly speculative, one possible explanation underlying this finding might be the existence of a Wnt-regulated

adipocyte factor that signals to the pancreas to suppress insulin secretion. When this signal is removed by impaired Wnt secretion from adipose tissue, elevated circulating insulin may act upon the liver to suppress gluconeogenesis, stimulate glycogen storage, and increase liver weight. Future quantitative measurements of regulated insulin secretion, glucose homeostasis, glycogen, and TAG in whole livers, as well as examination of hepatic cell size and number, may uncover mechanisms by which Wntless deficiency improves glucose tolerance in obese mice.

Consistent with our studies, adipocyte-specific β-catenin-deficient mice also exhibit decreased fat mass and improved glucose tolerance when fed long-term HFD [32]. In contrast, diet-induced obese *Tcf7l2*$^{-/-}$ mice demonstrate increased adipose tissue mass, impaired glucose tolerance, and greater insulin resistance [34]. The expression of a subset of lipogenic genes, including *Acly* and *Scd1*, is elevated in the WAT of these mice, in line with observed adipocyte hypertrophy, but counter to our results in cultured adipocytes and WAT from *Wls*$^{-/-}$ mice. The bases for these apparently conflicting results may include reported discrepancies between their RNAseq and qPCR results, generation of alternative splice variants with differential cis-element binding or transcriptional activity, or compensatory binding of other TCF/LEF transcription factors to cis-elements [107–110]. Alternatively, it is conceivable that there are distinctions between knockout of Wnt secretion and deletion of a downstream transcriptional effector of β-catenin; to this end, Tcf7l2 has also been shown to have transcriptional activity independent of β-catenin in certain contexts [111] and its deletion may therefore impact distinct pathways. Indeed, Geogheghan *et al.* reported that *Tcf7l2* deletion repressed the expression of lipolytic genes, possibly contributing to adipocyte hypertrophy and subsequent metabolic dysfunction on HFD. In any case, the results from both groups indicate that Wnt signaling regulates lipid metabolism in adipocytes.

In a gain-of-function Wnt signaling model, global *Sfrp5*^{Q27Stop} mice fed HFD are characterized by decreased adipocyte size and WAT mass, elevated mitochondrial variables including oxygen consumption, and a mild improvement in glucose homeostasis [33]. These effects of SFRP5 on glucose homeostasis are largely supported by the injection of SFRP5 neutralizing antibody [112]. Consistent with these data, transgenic mice with enforced expression of Wnt10b from the FABP4 promoter have less WAT when maintained on NCD, are resistant to HFD-induced or genetic obesity, and are more glucose tolerant and insulin sensitive than controls [13,14]. Taken together, these gain-of-function models support the hypothesis that increased adipose Wnt signaling influences whole-body glucose homeostasis; however, further research is required to establish mechanisms and to resolve differences in experimental outcomes.

In summary, we demonstrated that Wnt/β-catenin signaling is active in adipocytes and adipocyte-derived Wnts are required for the expression of a network of lipogenic genes. Further, adipocytes compensate for Wnt deficiency through cell-autonomous mechanisms, and WAT defends the loss of adipocyte-derived Wnts by upregulating Wnt signaling in SVCs. This compensatory mechanism for maintaining homeostasis is overridden by long-term HFD, revealing that *Wls*$^{-/-}$ mice are resistant to diet-induced obesity, adipocyte hypertrophy, and metabolic dysfunction.

ACKNOWLEDGEMENTS

This study was supported by grants from the NIH to OAM (RO1 DK62876 and R24 DK092759), DPB (T32 HD007505 and T32 GM007863), CAC (T32 DK101357), KTL (T32 DK071212 and F32 DK122654), RLS (T32 DK101357 and F32 DK123887), SMR (T32 GM835326 and F31 DK12272301), and the American Diabetes Association to ZL (1-18-PDF-087) and CAC (1-18-PDF-064). This research was also supported by core facilities, including the Michigan Mouse Metabolic Phenotyping Center (U2C DK110768), the Microscopy, Imaging, and Cellular Physiology Core (P30 DK020572), the Michigan Regional Comprehensive Metabolomics Resource Core (U24 DK097153), the Adipose Tissue Core of the MNORC (P30 DK089503), the University of Michigan Advanced Genomics Core, and the University of Michigan Proteomics and Peptide Synthesis Core.

CONFLICTS OF INTEREST

The authors have no conflicts of interest to report.

APPENDIX A. SUPPLEMENTARY DATA

Supplementary data to this article can be found online at https://doi.org/10.1016/j.molmet.2020.100992.

REFERENCES

[1] Cadigan, K.M., Nusse, R., 1997. Wnt signaling: a common theme in animal development. Genes & Development 11(24):3286–3305.
[2] Clevers, H., 2006. Wnt/beta-catenin signaling in development and disease. Cell 127(3):469–480.
[3] Clevers, H., Nusse, R., 2012. Wnt/beta-catenin signaling and disease. Cell 149(6):1192–1205.
[4] Prestwich, T.C., Macdougald, O.A., 2007. Wnt/beta-catenin signaling in adipogenesis and metabolism. Current Opinion in Cell Biology 19(6):612–617.
[5] Ross, S.E., Hemati, N., Longo, K.A., Bennett, C.N., Lucas, P.C., Erickson, R.L., et al., 2000. Inhibition of adipogenesis by Wnt signaling. Science 289(5481): 950–953.
[6] Bennett, C.N., Ross, S.E., Longo, K.A., Bajnok, L., Hemati, N., Johnson, K.W., et al., 2002. Regulation of Wnt signaling during adipogenesis. Journal of Biological Chemistry 277(34):30998–31004.
[7] Moldes, M., Zuo, Y., Morrison, R.F., Silva, D., Park, B.H., Liu, J., et al., 2003. Peroxisome-proliferator-activated receptor gamma suppresses Wnt/beta-catenin signalling during adipogenesis. Biochemical Journal 376(Pt 3): 607–613.
[8] Villanueva, C.J., Waki, H., Godio, C., Nielsen, R., Chou, W.L., Vargas, L., et al., 2011. TLE3 is a dual-function transcriptional coregulator of adipogenesis. Cell Metabolism 13(4):413–427.
[9] Christodoulides, C., Lagathu, C., Sethi, J.K., Vidal-Puig, A., 2009. Adipogenesis and WNT signalling. Trends in Endocrinology and Metabolism 20(1): 16–24.
[10] Sethi, J.K., Vidal-Puig, A., 2010. Wnt signalling and the control of cellular metabolism. Biochemical Journal 427(1):1–17.
[11] Lagathu, C., Christodoulides, C., Virtue, S., Cawthorn, W.P., Franzin, C., Kimber, W.A., et al., 2009. Dact1, a nutritionally regulated preadipocyte gene, controls adipogenesis by coordinating the Wnt/beta-catenin signaling network. Diabetes 58(3):609–619.
[12] Cawthorn, W.P., Bree, A.J., Yao, Y., Du, B., Hemati, N., Martinez-Santibanez, G., et al., 2012. Wnt6, Wnt10a and Wnt10b inhibit adipogenesis and stimulate osteoblastogenesis through a beta-catenin-dependent mechanism. Bone 50(2):477–489.
[13] Longo, K.A., Wright, W.S., Kang, S., Gerin, I., Chiang, S.H., Lucas, P.C., et al., 2004. Wnt10b inhibits development of white and brown adipose tissues. Journal of Biological Chemistry 279(34):35503–35509.
[14] Wright, W.S., Longo, K.A., Dolinsky, V.W., Gerin, I., Kang, S., Bennett, C.N., et al., 2007. Wnt10b inhibits obesity in ob/ob and agouti mice. Diabetes 56(2):295–303.

[15] Bennett, C.N., Longo, K.A., Wright, W.S., Suva, L.J., Lane, T.F., Hankenson, K.D., et al., 2005. Regulation of osteoblastogenesis and bone mass by Wnt10b. Proceedings of the National Academy of Sciences of the United States of America 102(9):3324–3329.

[16] Bennett, C.N., Ouyang, H., Ma, Y.L., Zeng, Q., Gerin, I., Sousa, K.M., et al., 2007. Wnt10b increases postnatal bone formation by enhancing osteoblast differentiation. Journal of Bone and Mineral Research 22(12):1924–1932.

[17] Kang, S., Bennett, C.N., Gerin, I., Rapp, L.A., Hankenson, K.D., Macdougald, O.A., 2007. Wnt signaling stimulates osteoblastogenesis of mesenchymal precursors by suppressing CCAAT/enhancer-binding protein alpha and peroxisome proliferator-activated receptor gamma. Journal of Biological Chemistry 282(19):14515–14524.

[18] Krishnan, V., Bryant, H.U., Macdougald, O.A., 2006. Regulation of bone mass by Wnt signaling. Journal of Clinical Investigation 116(5):1202–1209.

[19] Grant, S.F., Thorleifsson, G., Reynisdottir, I., Benediktsson, R., Manolescu, A., Sainz, J., et al., 2006. Variant of transcription factor 7-like 2 (TCF7L2) gene confers risk of type 2 diabetes. Nature Genetics 38(3):320–323.

[20] Lyssenko, V., Lupi, R., Marchetti, P., Del Guerra, S., Orho-Melander, M., Almgren, P., et al., 2007. Mechanisms by which common variants in the TCF7L2 gene increase risk of type 2 diabetes. Journal of Clinical Investigation 117(8):2155–2163.

[21] Jin, T., 2016. Current understanding on role of the Wnt signaling pathway effector TCF7L2 in glucose homeostasis. Endocrine Reviews 37(3):254–277.

[22] Saarinen, A., Saukkonen, T., Kivela, T., Lahtinen, U., Laine, C., Somer, M., et al., 2010. Low density lipoprotein receptor-related protein 5 (LRP5) mutations and osteoporosis, impaired glucose metabolism and hypercholesterolaemia. Clinical Endocrinology 72(4):481–488.

[23] Singh, R., Smith, E., Fathzadeh, M., Liu, W., Go, G.W., Subrahmanyan, L., et al., 2013. Rare nonconservative LRP6 mutations are associated with metabolic syndrome. Human Mutation 34(9):1221–1225.

[24] Loh, N.Y., Neville, M.J., Marinou, K., Hardcastle, S.A., Fielding, B.A., Duncan, E.L., et al., 2015. LRP5 regulates human body fat distribution by modulating adipose progenitor biology in a dose- and depot-specific fashion. Cell Metabolism 21(2):262–273.

[25] Shungin, D., Winkler, T.W., Croteau-Chonka, D.C., Ferreira, T., Locke, A.E., Magi, R., et al., 2015. New genetic loci link adipose and insulin biology to body fat distribution. Nature 518(7538):187–196.

[26] Heid, I.M., Jackson, A.U., Randall, J.C., Winkler, T.W., Qi, L., Steinthorsdottir, V., et al., 2010. Meta-analysis identifies 13 new loci associated with waist-hip ratio and reveals sexual dimorphism in the genetic basis of fat distribution. Nature Genetics 42(11):949–960.

[27] Hao, H.X., Xie, Y., Zhang, Y., Charlat, O., Oster, E., Avello, M., et al., 2012. ZNRF3 promotes Wnt receptor turnover in an R-spondin-sensitive manner. Nature 485(7397):195–200.

[28] Zou, Y., Ning, T., Shi, J., Chen, M., Ding, L., Huang, Y., et al., 2017. Association of a gain-of-function variant in LGR4 with central obesity. Obesity (Silver Spring) 25(1):252–260.

[29] Van Camp, J.K., Beckers, S., Zegers, D., Verrijken, A., Van Gaal, L.F., Van Hul, W., 2014. Common genetic variation in sFRP5 is associated with fat distribution in men. Endocrine 46(3):477–484.

[30] Christodoulides, C., Scarda, A., Granzotto, M., Milan, G., Dalla Nora, E., Keogh, J., et al., 2006. WNT10B mutations in human obesity. Diabetologia 49(4):678–684.

[31] Kanazawa, A., Tsukada, S., Sekine, A., Tsunoda, T., Takahashi, A., Kashiwagi, A., et al., 2004. Association of the gene encoding wingless-type mammary tumor virus integration-site family member 5B (WNT5B) with type 2 diabetes. The American Journal of Human Genetics 75(5):832–843.

[32] Chen, M., Lu, P., Ma, Q., Cao, Y., Chen, N., Li, W., et al., 2020. CTNNB1/beta-catenin dysfunction contributes to adiposity by regulating the cross-talk of mature adipocytes and preadipocytes. Science Advances 6(2): eaax9605.

[33] Mori, H., Prestwich, T.C., Reid, M.A., Longo, K.A., Gerin, I., Cawthorn, W.P., et al., 2012. Secreted frizzled-related protein 5 suppresses adipocyte mitochondrial metabolism through WNT inhibition. Journal of Clinical Investigation 122(7):2405–2416.

[34] Geoghegan, G., Simcox, J., Seldin, M.M., Parnell, T.J., Stubben, C., Just, S., et al., 2019. Targeted deletion of Tcf7l2 in adipocytes promotes adipocyte hypertrophy and impaired glucose metabolism. Molecular Metabolism 24: 44–63.

[35] Das, S., Yu, S., Sakamori, R., Stypulkowski, E., Gao, N., 2012. Wntless in Wnt secretion: molecular, cellular and genetic aspects. Frontier in Biology (Beijing) 7(6):587–593.

[36] Banziger, C., Soldini, D., Schutt, C., Zipperlen, P., Hausmann, G., Basler, K., 2006. Wntless, a conserved membrane protein dedicated to the secretion of Wnt proteins from signaling cells. Cell 125(3):509–522.

[37] Coombs, G.S., Yu, J., Canning, C.A., Veltri, C.A., Covey, T.M., Cheong, J.K., et al., 2010. WLS-dependent secretion of WNT3A requires Ser209 acylation and vacuolar acidification. Journal of Cell Science 123(Pt 19):3357–3367.

[38] Najdi, R., Proffitt, K., Sprowl, S., Kaur, S., Yu, J., Covey, T.M., et al., 2012. A uniform human Wnt expression library reveals a shared secretory pathway and unique signaling activities. Differentiation 84(2):203–213.

[39] Herr, P., Basler, K., 2012. Porcupine-mediated lipidation is required for Wnt recognition by Wls. Developmental Biology 361(2):392–402.

[40] Rios-Esteves, J., Haugen, B., Resh, M.D., 2014. Identification of key residues and regions important for porcupine-mediated Wnt acylation. Journal of Biological Chemistry 289(24):17009–17019.

[41] Rios-Esteves, J., Resh, M.D., 2013. Stearoyl CoA desaturase is required to produce active, lipid-modified Wnt proteins. Cell Rep 4(6):1072–1081.

[42] Takada, R., Satomi, Y., Kurata, T., Ueno, N., Norioka, S., Kondoh, H., et al., 2006. Monounsaturated fatty acid modification of Wnt protein: its role in Wnt secretion. Developmental Cell 11(6):791–801.

[43] Sun, J., Yu, S., Zhang, X., Capac, C., Aligbe, O., Daudelin, T., et al., 2017. A Wntless-SEC12 complex on the ER membrane regulates early Wnt secretory vesicle assembly and mature ligand export. Journal of Cell Science 130(13):2159–2171.

[44] Carpenter, A.C., Rao, S., Wells, J.M., Campbell, K., Lang, R.A., 2010. Generation of mice with a conditional null allele for Wntless. Genesis 48(9):554–558.

[45] Fu, J., Jiang, M., Mirando, A.J., Yu, H.M., Hsu, W., 2009. Reciprocal regulation of Wnt and Gpr177/mouse Wntless is required for embryonic axis formation. Proceedings of the National Academy of Sciences of the United States of America 106(44):18598–18603.

[46] Preziosi, M., Okabe, H., Poddar, M., Singh, S., Monga, S.P., 2018. Endothelial Wnts regulate beta-catenin signaling in murine liver zonation and regeneration: a sequel to the Wnt-Wnt situation. Hepatology Communications 2(7): 845–860.

[47] Zhong, Z., Zylstra-Diegel, C.R., Schumacher, C.A., Baker, J.J., Carpenter, A.C., Rao, S., et al., 2012. Wntless functions in mature osteoblasts to regulate bone mass. Proceedings of the National Academy of Sciences of the United States of America 109(33):E2197–E2204.

[48] Jiang, M., Ku, W.Y., Fu, J., Offermanns, S., Hsu, W., Que, J., 2013. Gpr177 regulates pulmonary vasculature development. Development 140(17):3589–3594.

[49] Cornett, B., Snowball, J., Varisco, B.M., Lang, R., Whitsett, J., Sinner, D., 2013. Wntless is required for peripheral lung differentiation and pulmonary vascular development. Developmental Biology 379(1):38–52.

[50] Zhu, X., Zhu, H., Zhang, L., Huang, S., Cao, J., Ma, G., et al., 2012. Wls-mediated Wnts differentially regulate distal limb patterning and tissue morphogenesis. Developmental Biology 365(2):328–338.

[51] Shao, W., Espenshade, P.J., 2012. Expanding roles for SREBP in metabolism. Cell Metabolism 16(4):414–419.

[52] Horton, J.D., Goldstein, J.L., Brown, M.S., 2002. SREBPs: activators of the complete program of cholesterol and fatty acid synthesis in the liver. Journal of Clinical Investigation 109(9):1125–1131.

[53] Iizuka, K., Bruick, R.K., Liang, G., Horton, J.D., Uyeda, K., 2004. Deficiency of carbohydrate response element-binding protein (ChREBP) reduces lipogenesis as well as glycolysis. Proceedings of the National Academy of Sciences of the United States of America 101(19):7281–7286.

[54] Mancini, R., Noto, A., Pisanu, M.E., De Vitis, C., Maugeri-Sacca, M., Ciliberto, G., 2018. Metabolic features of cancer stem cells: the emerging role of lipid metabolism. Oncogene 37(18):2367–2378.

[55] Mauvoisin, D., Charfi, C., Lounis, A.M., Rassart, E., Mounier, C., 2013. Decreasing stearoyl-CoA desaturase-1 expression inhibits beta-catenin signaling in breast cancer cells. Cancer Science 104(1):36–42.

[56] Fritz, V., Benfodda, Z., Rodier, G., Henriquet, C., Iborra, F., Avances, C., et al., 2010. Abrogation of de novo lipogenesis by stearoyl-CoA desaturase 1 inhibition interferes with oncogenic signaling and blocks prostate cancer progression in mice. Molecular Cancer Therapeutics 9(6):1740–1754.

[57] Pisanu, M.E., Noto, A., De Vitis, C., Morrone, S., Scognamiglio, G., Botti, G., et al., 2017. Blockade of Stearoyl-CoA-desaturase 1 activity reverts resistance to cisplatin in lung cancer stem cells. Cancer Letters 406:93–104.

[58] Dai, S., Yan, Y., Xu, Z., Zeng, S., Qian, L., Huo, L., et al., 2017. SCD1 confers temozolomide resistance to human glioma cells via the akt/GSK3beta/beta-catenin signaling Axis. Frontiers in Pharmacology 8:960.

[59] Zhou, Z., Lu, Y., Wang, Y., Du, L., Zhang, Y., Tao, J., 2019. Let-7c regulates proliferation and osteodifferentiation of human adipose-derived mesenchymal stem cells under oxidative stress by targeting SCD-1. American Journal of Physiology - Cell Physiology 316(1):C57–C69.

[60] Jazurek-Ciesiolka, M., Janikiewicz, J., Dobrzyn, P., Dziewulska, A., Kozinski, K., Dobrzyn, A., 2019. Oleic acid increases the transcriptional activity of FoxO1 by promoting its nuclear translocation and beta-catenin binding in pancreatic beta-cells. Biochimica et Biophysica Acta - Molecular Basis of Disease 1865(10):2753–2764.

[61] Ma, X.L., Sun, Y.F., Wang, B.L., Shen, M.N., Zhou, Y., Chen, J.W., et al., 2019. Sphere-forming culture enriches liver cancer stem cells and reveals Stearoyl-CoA desaturase 1 as a potential therapeutic target. BMC Cancer 19(1):760.

[62] Bagchi, D.P., MacDougald, O.A., 2019. Identification and dissection of diverse mouse adipose depots. Journal of Visualized Experiments 149.

[63] Bagchi, D.P., Forss, I., Mandrup, S., MacDougald, O.A., 2018. SnapShot: niche determines adipocyte character I. Cell Metabolism 27(1):264–264 e261.

[64] Parlee, S.D., Lentz, S.I., Mori, H., MacDougald, O.A., 2014. Quantifying size and number of adipocytes in adipose tissue. Methods in Enzymology 537:93–122.

[65] Rim, J.S., Mynatt, R.L., Gawronska-Kozak, B., 2005. Mesenchymal stem cells from the outer ear: a novel adult stem cell model system for the study of adipogenesis. The FASEB Journal 19(9):1205–1207.

[66] Gawronska-Kozak, B., 2014. Preparation and differentiation of mesenchymal stem cells from ears of adult mice. Methods in Enzymology 538:1–13.

[67] Erickson, R.L., Hemati, N., Ross, S.E., MacDougald, O.A., 2001. p300 coactivates the adipogenic transcription factor CCAAT/enhancer-binding protein alpha. Journal of Biological Chemistry 276(19):16348–16355.

[68] Young, C.S., Kitamura, M., Hardy, S., Kitajewski, J., 1998. Wnt-1 induces growth, cytosolic beta-catenin, and Tcf/Lef transcriptional activation in Rat-1 fibroblasts. Molecular and Cellular Biology 18(5):2474–2485.

[69] Scheller, E.L., Doucette, C.R., Learman, B.S., Cawthorn, W.P., Khandaker, S., Schell, B., et al., 2015. Region-specific variation in the properties of skeletal adipocytes reveals regulated and constitutive marrow adipose tissues. Nature Communications 6:7808.

[70] Lengfeld, J.E., Lutz, S.E., Smith, J.R., Diaconu, C., Scott, C., Kofman, S.B., et al., 2017. Endothelial Wnt/beta-catenin signaling reduces immune cell infiltration in multiple sclerosis. Proceedings of the National Academy of Sciences of the United States of America 114(7):E1168–E1177.

[71] Boulter, L., Govaere, O., Bird, T.G., Radulescu, S., Ramachandran, P., Pellicoro, A., et al., 2012. Macrophage-derived Wnt opposes Notch signaling to specify hepatic progenitor cell fate in chronic liver disease. Nature Medicine 18(4):572–579.

[72] Chakrabarti, R., Celia-Terrassa, T., Kumar, S., Hang, X., Wei, Y., Choudhury, A., et al., 2018. Notch ligand Dll1 mediates cross-talk between mammary stem cells and the macrophageal niche. Science 360(6396).

[73] Nusse, R., Clevers, H., 2017. Wnt/beta-Catenin signaling, disease, and emerging therapeutic modalities. Cell 169(6):985–999.

[74] Miller, J.R., Moon, R.T., 1997. Analysis of the signaling activities of localization mutants of beta-catenin during axis specification in Xenopus. The Journal of Cell Biology 139(1):229–243.

[75] Sampath, H., Ntambi, J.M., 2011. The role of stearoyl-CoA desaturase in obesity, insulin resistance, and inflammation. Annals of the New York Academy of Sciences 1243:47–53.

[76] Paton, C.M., Ntambi, J.M., 2009. Biochemical and physiological function of stearoyl-CoA desaturase. American Journal of Physiology. Endocrinology and Metabolism 297(1):E28–E37.

[77] Ameer, F., Scandiuzzi, L., Hasnain, S., Kalbacher, H., Zaidi, N., 2014. De novo lipogenesis in health and disease. Metabolism 63(7):895–902.

[78] Sanders, F.W., Griffin, J.L., 2016. De novo lipogenesis in the liver in health and disease: more than just a shunting yard for glucose. Biological Reviews of the Cambridge Philosophical Society 91(2):452–468.

[79] Ralston, J.C., Badoud, F., Cattrysse, B., McNicholas, P.D., Mutch, D.M., 2014. Inhibition of stearoyl-CoA desaturase-1 in differentiating 3T3-L1 preadipocytes upregulates elongase 6 and downregulates genes affecting triacylglycerol synthesis. International Journal of Obesity 38(11):1449–1456.

[80] Wang, Y., Viscarra, J., Kim, S.J., Sul, H.S., 2015. Transcriptional regulation of hepatic lipogenesis. Nature Reviews Molecular Cell Biology 16(11):678–689.

[81] Tian, J., Goldstein, J.L., Brown, M.S., 2016. Insulin induction of SREBP-1c in rodent liver requires LXRalpha-C/EBPbeta complex. Proceedings of the National Academy of Sciences of the United States of America 113(29):8182–8187.

[82] Linden, A.G., Li, S., Choi, H.Y., Fang, F., Fukasawa, M., Uyeda, K., et al., 2018. Interplay between ChREBP and SREBP-1c coordinates postprandial glycolysis and lipogenesis in livers of mice. The Journal of Lipid Research 59(3):475–487.

[83] Yabe, D., Komuro, R., Liang, G., Goldstein, J.L., Brown, M.S., 2003. Liver-specific mRNA for Insig-2 downregulated by insulin: implications for fatty acid synthesis. Proceedings of the National Academy of Sciences of the United States of America 100(6):3155–3160.

[84] Carobbio, S., Hagen, R.M., Lelliott, C.J., Slawik, M., Medina-Gomez, G., Tan, C.Y., et al., 2013. Adaptive changes of the Insig1/SREBP1/SCD1 set point help adipose tissue to cope with increased storage demands of obesity. Diabetes 62(11):3697–3708.

[85] Crewe, C., Zhu, Y., Paschoal, V.A., Joffin, N., Ghaben, A.L., Gordillo, R., et al., 2019. SREBP-regulated adipocyte lipogenesis is dependent on substrate availability and redox modulation of mTORC1. JCI Insight 5.

[86] Matsuda, M., Korn, B.S., Hammer, R.E., Moon, Y.A., Komuro, R., Horton, J.D., et al., 2001. SREBP cleavage-activating protein (SCAP) is required for increased lipid synthesis in liver induced by cholesterol deprivation and insulin elevation. Genes & Development 15(10):1206–1216.

[87] Yabe, D., Brown, M.S., Goldstein, J.L., 2002. Insig-2, a second endoplasmic reticulum protein that binds SCAP and blocks export of sterol regulatory element-binding proteins. Proceedings of the National Academy of Sciences of the United States of America 99(20):12753–12758.

[88] Jeffery, E., Berry, R., Church, C.D., Yu, S., Shook, B.A., Horsley, V., et al., 2014. Characterization of Cre recombinase models for the study of adipose tissue. Adipocyte 3(3):206–211.

[89] Mukohira, H., Hara, T., Abe, S., Tani-Ichi, S., Sehara-Fujisawa, A., Nagasawa, T., et al., 2019. Mesenchymal stromal cells in bone marrow

express adiponectin and are efficiently targeted by an adiponectin promoter-driven Cre transgene. International Immunology 31(11):729—742.

[90] Li, Z., Hardij, J., Bagchi, D.P., Scheller, E.L., MacDougald, O.A., 2018. Development, regulation, metabolism and function of bone marrow adipose tissues. Bone 110:134—140.

[91] Kennell, J.A., MacDougald, O.A., 2005. Wnt signaling inhibits adipogenesis through beta-catenin-dependent and -independent mechanisms. Journal of Biological Chemistry 280(25):24004—24010.

[92] Li, F.Q., Singh, A.M., Mofunanya, A., Love, D., Terada, N., Moon, R.T., et al., 2007. Chibby promotes adipocyte differentiation through inhibition of beta-catenin signaling. Molecular and Cellular Biology 27(12):4347—4354.

[93] Grunberg, J.R., Hoffmann, J.M., Hedjazifar, S., Nerstedt, A., Jenndahl, L., Elvin, J., et al., 2017. Overexpressing the novel autocrine/endocrine adipokine WISP2 induces hyperplasia of the heart, white and brown adipose tissues and prevents insulin resistance. Scientific Reports 7:43515.

[94] Murahovschi, V., Pivovarova, O., Ilkavets, I., Dmitrieva, R.M., Docke, S., Keyhani-Nejad, F., et al., 2015. WISP1 is a novel adipokine linked to inflammation in obesity. Diabetes 64(3):856—866.

[95] Christodoulides, C., Laudes, M., Cawthorn, W.P., Schinner, S., Soos, M., O'Rahilly, S., et al., 2006. The Wnt antagonist Dickkopf-1 and its receptors are coordinately regulated during early human adipogenesis. Journal of Cell Science 119(Pt 12):2613—2620.

[96] Wiese, K.E., Nusse, R., van Amerongen, R., 2018. Wnt signalling: conquering complexity. Development 145(12).

[97] Jho, E.H., Zhang, T., Domon, C., Joo, C.K., Freund, J.N., Costantini, F., 2002. Wnt/beta-catenin/Tcf signaling induces the transcription of Axin2, a negative regulator of the signaling pathway. Molecular and Cellular Biology 22(4): 1172—1183.

[98] Ross, S.E., Erickson, R.L., Gerin, I., DeRose, P.M., Bajnok, L., Longo, K.A., et al., 2002. Microarray analyses during adipogenesis: understanding the effects of Wnt signaling on adipogenesis and the roles of liver X receptor alpha in adipocyte metabolism. Molecular and Cellular Biology 22(16):5989—5999.

[99] ten Berge, D., Brugmann, S.A., Helms, J.A., Nusse, R., 2008. Wnt and FGF signals interact to coordinate growth with cell fate specification during limb development. Development 135(19):3247—3257.

[100] Nakashima, A., Katagiri, T., Tamura, M., 2005. Cross-talk between Wnt and bone morphogenetic protein 2 (BMP-2) signaling in differentiation pathway of C2C12 myoblasts. Journal of Biological Chemistry 280(45):37660—37668.

[101] Bertrand, F.E., Angus, C.W., Partis, W.J., Sigounas, G., 2012. Developmental pathways in colon cancer: crosstalk between WNT, BMP, Hedgehog and Notch. Cell Cycle 11(23):4344—4351.

[102] Soshnikova, N., Zechner, D., Huelsken, J., Mishina, Y., Behringer, R.R., Taketo, M.M., et al., 2003. Genetic interaction between Wnt/beta-catenin and BMP receptor signaling during formation of the AER and the dorsal-ventral axis in the limb. Genes & Development 17(16):1963—1968.

[103] Carobbio, S., Pellegrinelli, V., Vidal-Puig, A., 2017. Adipose tissue function and expandability as determinants of lipotoxicity and the metabolic syndrome. Advances in Experimental Medicine & Biology 960:161—196.

[104] Qatanani, M., Lazar, M.A., 2007. Mechanisms of obesity-associated insulin resistance: many choices on the menu. Genes & Development 21(12):1443—1455.

[105] Kusminski, C.M., Bickel, P.E., Scherer, P.E., 2016. Targeting adipose tissue in the treatment of obesity-associated diabetes. Nature Reviews Drug Discovery 15(9):639—660.

[106] Bagchi, D.P., Forss, I., Mandrup, S., MacDougald, O.A., 2018. SnapShot: niche determines adipocyte character II. Cell Metab 27(1):264—264 e261.

[107] Weise, A., Bruser, K., Elfert, S., Wallmen, B., Wittel, Y., Wohrle, S., et al., 2010. Alternative splicing of Tcf7l2 transcripts generates protein variants with differential promoter-binding and transcriptional activation properties at Wnt/beta-catenin targets. Nucleic Acids Research 38(6):1964—1981.

[108] Chen, X., Ayala, I., Shannon, C., Fourcaudot, M., Acharya, N.K., Jenkinson, C.P., et al., 2018. The diabetes gene and Wnt pathway effector TCF7L2 regulates adipocyte development and function. Diabetes 67(4):554—568.

[109] Kennell, J.A., O'Leary, E.E., Gummow, B.M., Hammer, G.D., MacDougald, O.A., 2003. T cell factor 4N (TCF-4N), a novel isoform of mouse TCF-4, synergizes with beta-catenin to coactivate C/EBPalpha and steroidogenic factor 1 transcription factors. Molecular and Cellular Biology 23(15):5366—5375.

[110] Cristancho, A.G., Schupp, M., Lefterova, M.I., Cao, S., Cohen, D.M., Chen, C.S., et al., 2011. Repressor transcription factor 7-like 1 promotes adipogenic competency in precursor cells. Proceedings of the National Academy of Sciences of the United States of America 108(39):16271—16276.

[111] Hammond, E., Lang, J., Maeda, Y., Pleasure, D., Angus-Hill, M., Xu, J., et al., 2015. The Wnt effector transcription factor 7-like 2 positively regulates oligodendrocyte differentiation in a manner independent of Wnt/beta-catenin signaling. Journal of Neuroscience 35(12):5007—5022.

[112] Rulifson, I.C., Majeti, J.Z., Xiong, Y., Hamburger, A., Lee, K.J., Miao, L., et al., 2014. Inhibition of secreted frizzled-related protein 5 improves glucose metabolism. American Journal of Physiology. Endocrinology and Metabolism 307(12):E1144—E1152.

